# ADDIS ABABA UNIVERSITY

# SCHOOL OF GRADUATE STUDIES

# ADDIS ABABA INSTITUTE OF TECHNOLOGY

# SCHOOL OF CIVIL AND ENVIRONMETAL ENGINEERING



## Experimental Study in to Passive Auto-Tuning Compound Pendulum Mass Damper.


**By**

**Yirga Terefe.**


**A Research Report Submitted to School of Graduate Studies in Partial Fulfilment of Master of Science in Civil Engineering (Structural Engineering).**

**Advisor: Dr. Abrham Gebre.**

February 2020

Addis Ababa, Ethiopia

**Addis Ababa University**

**Addis Ababa institute of Technology**

**School of Graduate Studies**

**Experimental Study in to Passive Auto-Tuning Compound Pendulum Mass Damper.**

**By**

**Yirga Terefe.**

## Approved by the board of examiners.

| | | | |
|---|---|---|---|
| 1. | DR. ABRHAM GEBRE.<br>Advisor | _____<br>Signature | _____<br>Date |
| 2. | DR. ING. ADIL ZEKARIA.<br>Internal examiner | _____<br>Signature | _____<br>Date |
| 3. | DR. ING. ESAYAS G/YOHANNES.<br>External examiner | _____<br>Signature | _____<br>Date |
| 4. | CHAIRPERSON | _____<br>Signature | _____<br>Date |

# DECLARATION.

I, the undersigned, declare that this thesis entitled "*Experimental Study in to Passive Auto-Tuning Compound Pendulum Mass Damper*" is my original work. This thesis has not been presented for any other university and is not concurrently submitted in candidature of any other degree, and that all sources of material used for the thesis have been duly acknowledged.

Name: Yirga Terefe.

Signature: _____

Place: Addis Ababa Institute of Technology, AAU, Ethiopia

Date of Submission: February, 2020

# ABSTRACT

Now a days, the numbers of taller and lighter structures are continuously increasing in the construction industries which are flexible and having a very low damping value. Those structures can easily fail under structural vibrations induced by earthquake and wind. Therefore several techniques are available today to minimize the vibration of the structure, out of which concept of using Passive auto-tuning compound pendulum mass damper (PATCPMD) is a newer one. There are in general large numbers of studies on theoretical investigation of behaviour of buildings with tuned mass dampers under various impacts. However, the experimental studies in this area are quite limited. In this thesis, A two-story steel test model structure was used to carry out the experimental study. The PATCPMD was suspended first in the upper and second in the lower story of the structure to be controlled by a group of ropes in the manner that they form compound pendulum but not exactly a compound pendulum and was free to move in any translational direction.

First, the PATCPMD efficiency tests was carried out, whereby the test model was subjected to translational, torsional and coupled free vibration tests and translational forced harmonic vibration tests, initially without the PATCPMD and then with the PATCPMD at different story of the primary model structure, in order to determine the damping effects of the PATCPMD and to determine the better effect of the PATCPMD with respect to location. The results demonstrate that it is capable of providing significant control of translational, torsional and coupled vibrations of the structure without being tuned in both cases. However, a better effect was observed when the PATCPMD was suspended on the second story.

Secondly, Once the better effect of the PATCPMD with respect to location was determined, a parameter study was carried out whereby the dynamic properties of the primary test model was varied whilst the PATCPMD is left unchanged. The free and forced vibration tests were repeated, without any tuning of the system taking place. Furthermore, the result demonstrates the PATCPMD's effectiveness under different conditions of the system, without having undergone any tuning. Finally, the PATCPMD was suspended on to the test model on three different connection patterns so as to investigate the better effect out of them. Again a positive results were obtained with this regard. However, pattern 1 has got a better efficiency among the others two. In general the study shows that the PATCPMD is robust, simple and versatile making it an ideal application for engineering structures.

# ACKNOWLEDGEMENTS.

I express my deepest gratitude to my advisor, **Dr. Abrham Gebre** for his support, encouragement, expert guidance and patience throughout this study. I would also like to thank **Mr. Tekleye Geda** for his continuous support for my thesis from the beginning up to the end and other laboratory staff at the Civil, Mechanical and Electrical Engineering Department at Ambo University for their help in setting up my test model for my research.

Finally unconditional love, support and encouragement of my family to continue my effort in difficult times was wonderful. They deserve much love and thanks.

**TABLE OF CONTENTS.** **PAGES**

**LIST OF FIGURES.**

# Chapter 1.

# INTRODUCTION

## 1.1. General.

The use of high strength materials and the development of new building techniques have reduced the cost of modern structures to a great extent, but at the same time caused modern structures to be more flexible and lightly damped than in the past. The rapid and historic growth of urbanization also created a surge in the construction of high-rise buildings. Such structures are inherently sensitive to earthquake or wind excitation. Consequently, induced oscillations of structures due to earthquake and wind may cause human discomfort, cracked partitions, broken glass, damaged sensitive equipments and even catastropic failure of some bridges and towers. As a result vibration control of structural system in order to provide safety and functionality against induced vibration has always been considered as major relevant technological challenges for the designers.

To ensure functional performance of structures it is important to reduce undesirable structural vibrations under earthquake and wind loading. Various possibilities exist to achieve this goal, which include structural modification, aerodynamic modification and use of control technology. The use of passive or active control technology, however, is gaining wide acceptance in the building industry as evidenced by recent implementation of control devices on tall buildings and other flexible structures. In fact, we are entering a new era, leaving behind the days in which buildings and structures only offered space or a single function, to an era of providing an environment of comfort, multi-function services, high-level communication network systems and highly efficient productivity. Hence, control systems, either active or passive, will become an integral part of structural systems. It has also been predicted that the realization of control technology in civil engineering may cause a revolution in this field.

A number of technologies have been invented and adopted to control excessive vibration and to reduce structural response and keep it within tolerable limit during unexpected events like earthquake. Primarily vibration control devices can be classified into passive, active and hybrid control systems. The technologies commonly adopted to control vibration in order to minimize damage and improve structural performance include damping, vibration isolation, control of excitation forces, vibration absorber and so forth. Each system has limitations and advantages in different perspective. The selection of a particular control system and technique is governed by a number of factors such as effectiveness, convenience, life cycle costs and so on. Among vibration absorbers Tuned Mass Damper (TMD), Active Mass Damper

(AMD), Hybrid Mass Damper (HBD) have been studied and installed in high rise buildings to control their behaviour under excitations. Among these systems still TMD is popular due to its simple principle and a number of successful applications in recent days.

In relatively recent years, the research of vibration control on Civil Engineering structures has increased with the development of active and passive control devices. Passive control devices are those which are activated by the excitation of the structure and possess no feedback capability. They seem to be favoured due to the fact that they do not require power for their use as well as their mechanical simplicity and efficiency. A common passive control device which is frequently featured in the literature is the Tuned Mass Damper (TMD). The World Trade Center Towers (1973) in New York and the John Hancock Tower (1976) in Boston were among the first practical applications of this type of control device. Since then, a number of high-rise buildings, towers, bridges, chimneys and mast structures have been fitted with a TMD in order to suppress wind induced vibrations.

Although TMDs have achieved a great amount of success, the main shortfall of their use is their need to be tuned to a particular modal frequency and the fact that their efficiency depends strictly on this frequency. Unfortunately, the structure's frequencies can change with time due to changes in the building's use or occupancy and changes to non-structural elements. These modifications may adjust the building's mass or stiffness and therefore alter its modal frequencies. Furthermore, errors in predicting the natural frequency of the structure are inevitable as well as inaccuracies in the fabrication of the TMD.

In general TMDs have been widely successful in many applications around the world However they possess two main shortfalls, their sensitivity to detuning and their lack of efficiency in controlling torsional and coupled vibration. For this reason, a passive auto-tuning Compound pendulum mass damper (PATCPMD) is proposed, which aims to eliminate these shortcomings and create a vibration control device which is simple, yet also feasible and effective.

### 1.2. Objectives of the Study.

A TMD is used only to control one frequency of the structure i.e. the frequency to which it has been tuned. However, a real structure will clearly contain more than one natural frequency as it can vibrate in a few translational directions (all with different frequencies), as well as in torsional and coupled directions (also with separate frequencies). Theoretically, each frequency to be controlled would require its own TMD.

Hence the study has the following objectives.

**General objective:**

The general objective of this research is to experimentally study two story steel floor system model to come up with a passive vibration control device which can control more than one frequency of the structure.

**Specific objectives:**

The specific objectives of the research are:

1. to experimentally investigate the PATCPMD's efficiency, in order to evaluate the PATCPMD's effectiveness at controlling vibration and attenuating the response of the test structure by suspending it at different stories of the Steel floor system model structure in controlling translational, torsional and coupled vibration.
2. to carry out parametric test in order to evaluate its robustness against detuning.

### 1.3. Significance of the Study.

It is well accepted that earthquakes and wind will continue to occur, and cause significant social, structural and economic damage if we are not prepared. Assessing earthquake and wind risk and improving engineering strategies to mitigate damage are thus the only viable options to create more resilient cities and communities. Geologists, seismologists and engineers are continuing their efforts to improve zoning maps, create reliable databases of earthquake processes and their effects, increase understanding of site characteristics, and develop earthquake resistant designs. As for the engineer, the ultimate goal is to design damage free, cost effective structures that will behave in a predictable and acceptable manner to maximise life safety and minimise damage.

Today, we understand to a great deal about how our built environment will respond to a wide range of earthquake motions. The challenges are therefore to develop new techniques and to improve on the existing practices so that the performance of these structures is predictable and acceptable. Hence with this regard the proposed research will contribute in the development and improvement of new techniques on the existing practices in controlling vibrations so that acceptable minimal or no damage will occur during earthquake and wind.

## 1.4. Layout of the Presentation.

As a general introduction to the thesis, this chapter indicates the background of the research, outlines the objectives of the research and points out the significance of the proposed thesis.

Chapter 2 contains the 'Literature Review', which presents a general summary of the literature that is available on a number of different types of vibration control devices that have been developed.

Chapter 3 contains the 'Experimental Methods', which outlines the various processes that were undertaken in carrying out this research. An introduction to TMDs followed by the experimental structure and setup used for the tests, as well as the experimental procedure was discussed.

Chapters 4 'Experimental Tests' contain the Results and Discussion, which present the results in graphical form, as well as summarising the outcomes of the experimental tests and discussing any observations.

Chapters 5 contain the 'Conclusions and Recommendations', which summarises the findings that can be drawn from the experimental test results and lists a few areas of the study which should be investigated further as recommendations.

# Chapter 2.
# LITERATURE REVIEW.

## 2.1. Literature Review.

Till date TMD has been studied by many researchers. The thought of TMD was first used by Frahm in 1909 to diminish the undulating motion of ships as well as ship hull vibrations. Later Hartog in 1940 developed analytical model for vibration controlling power of TMD. Later he optimized TMDs parameter for sinusoidal excitations. Fahim et al. (1997) considered different parameters like mass ratio, frequency ratio, damping ratio etc to obtain the optimum parameters which are used to compute the response of various single degree of freedom and multi degree of freedom structures with TMD at different earthquake excitation. The optimum parameters obtained are helpful in reducing the displacement and acceleration response significantly.

Wu et al. (1999) considered soil structure interaction in seismic response of tuned mass damper when fixed on a flexible based structure. A frequency independent model is used which covers a wide range of soil and structural characteristics. A stationary excitation is given to the model structure and the responses are used to measure the performance of TMD. It was observed that strong soil structure interaction considerably defeats the seismic effectiveness of TMD systems. Reduction in maximum response of the structure reduces with decrease in soil shear wave velocity. For any structure over soft soil, TMD structure is less effective in reducing the response due to high damping characteristics of soil structure system. The model is also subjected to NS component of the 1940 El Centro, California earthquake to observe the effectiveness of TMD in a realistic environment.

Nagashima et al. (2001) developed a hybrid mass damper (HMD) and applied it to a 36 storey high rise building with a bi-axial eccentricity, located in Tokyo. The system employs a gear type pendulum which make the natural period of the auxiliary mass relatively long while minimizing the height of the device and a linear actuator which ensures smooth and noiseless operation of the system. Transverse torsion coupled vibration is controlled by two HMD systems and various feedback control techniques has been developed to consume the capacity of HMD system for any external excitation. Free vibration tests as well as control of wind vibrations of the building induced by the Typhoon 9810 in 1998 were used to verify the performance of the control system. It was observed that the acceleration responses of the building were reduced to 63% and 47% of the corresponding uncontrolled accelerations.

Setareh (2001) studied the application of semi-active tuned mass dampers to base excitation systems. A single-degree-of-freedom system was subjected to sinusoidal base excitations and a damper was used to reduce the vibration. A new class of damper known as ground hook tuned mass damper (GHTMD) was used and optimum design parameters were obtained based on the minimization of steady state amplitude response of the main structure for different mass ratio and damping ratio. Frequency response was compared with and without TMD. In this paper, a design guide was presented based on non dimensional values to find optimum parameters of GHTMD.

Li and Liu (2002) manufactured an active multiple tuned mass damper (AMTMD) for structures subjected to ground acceleration keeping the stiffness and damping constant and varying the mass. Vibration in the structure is controlled by mode reduced order method. A numerical searching technique is used to demarcate the effect of optimum dynamic parameters on the strength of AMTMD. The parameters include the frequency spacing, damping ratio and frequency ratio and acceleration feedback gain coefficient. They compare the results of MTMD and AMTMD and concluded that it can effectively reduce the vibration of the structure underground acceleration. The AMTMD can also increase the performance of MTMD and more effective than ATMD.

Samali et al. (2003) described a five storey model using an active tuned mass damper by Fuzzy Logic Controller and linear quadratic regulator under earthquake excitation and a comparison is made. The effect of mass ratio and frequency ratio is conducted using fuzzy controller because of its ability to handle any non linear behaviour of the structure.

Chen and Wu (2003) numerically observed the effect of multiple tuned mass damper (MTMD) and compared the results with tuned mass damper (TMD). A three storey building frame was subjected to white noise excitation and tested in shake table. The results observed that multiple tuned mass dampers are more effective than tuned mass dampers in reducing the floor acceleration. The experimental and numerical results are compared and dynamic properties of the structure are validated successfully.

Li (2003) numerically observed the performance of multiple active-passive tuned mass dampers (MAPTMD) to prevent vibration of single degree of freedom structures subjected to ground acceleration with a uniform distribution of natural frequency. The MAPTMD generates a controlling force by keeping the displacement and velocity response gain and changing the acceleration response gain. Conclusion has been made that maximum tuning frequency ratio of MAPTMD decreases with increasing mass ratio and the effectiveness increases with the increase in mass ratio.

Ghosha and Basu (2004) observed the effect of soil structure interaction and concluded that when the soil becomes stiff, it allows the foundation to move relative to the surrounding soil which changes the soil foundation system from that of the fixed base. In such a case a conventional TMD loses its effectiveness in controlling the response of the structure to base excitation. So to avoid the effect of SSI, it is necessary to tune the damper to the fundamental frequency of the structure–foundation system. It is also essential to provide damping in the TMD greater than the critical damping to ensure response reduction of the structure.

Chouw (2004) studied the behavior of soil structure interaction with tuned mass dampers during near source earthquake at two different places varying the natural frequency of the dampers. They used the ground motions at the stations SCG and NRG of the 1994 Northridge earthquake for their study and concluded that soil structure interaction and ground motion can increase or decrease the effect of TMD.

Kwok and Samali (2006) carried out some experimental verifications of both active and passive TMD and compare the results with parametric study which are very useful in selection of optimal TMD parameters. 40-50% reduction in wind induced response & an additional damping of 3-4% of critical damping by using passive system and 2/3rd reduction in wind induced response & an additional damping of 10% of critical damping by using active system was obtained from their experimental investigation.

Saidi et al. (2007) developed a Tuned mass damper using viscoelastic material and concluded that TMD is effective when tuned to the natural frequency over a narrow band. They also describe the process of estimation of viscous damping of a damper made up of viscoelastic material. For any given floor mass, damping and stiffness a damper can be an economical and simple solution for retrofitting floors with excessive vibrations.

Wong (2008) studied dissipation of seismic energy in inelastic structures with tuned mass dampers. By using the force analogy method, an inelastic structure is modeled which is chosen as the base of plastic energy dissipation analysis in the structure. Energy response reduction after using TMD is also studied by using plastic energy spectra for various levels of structural yielding. The use of TMD increases the capacity of the structure to accumulate huge amounts of energy inside the TMD that will be released afterward in the form of damping energy. It reduces the plastic energy dissipation and increases the damping energy dissipation.

Alexander and Schilder (2009) proposed the performance of nonlinear tuned mass damper. A two degree of freedom system with a cubic nonlinearity is modeled. The nonlinearity is

originated from geometric arrangement of two pairs of springs. One pair helps in providing linear stiffness whereas the other pair rotates as they extend and helps in hardening spring stiffness. In this paper a software AUTO has been used to study numerically the periodic response of a nonlinear tuned mass damper and the optimum design parameters has been observed.

Lourenco et al.(2009) performed some experimental work taking a pendulum tuned mass damper with advantageous over conventional TMD. They did some simulation study considering the three dimensional behaviour of pendulum mass and found that the frequency can be re tuned by changing the cable length.

Lin et al.(2010) studied the vibration control of seismic structures using semi-active friction multiple tuned mass dampers. In this paper a semi active friction type multiple tuned mass damper (SAF-MTMD) is developed to control vibration in seismic structures. Since a friction type mass damper is same as a conventional mass damper if the static frictional force inactivates the mass damper. Various friction mechanisms have been used to activate all the mass units of friction type multiple tuned mass damper during earthquake. A comparison study is made with a passive friction type multiple tuned mass dampers and concluded that SAF-MTMD effectively reduces the seismic motion particularly at a larger intensity.

Islam and Ahsan (2012) optimized Tuned mass damper parameters using evolutionary operation algorithm and determined the optimum parameters of TMD in reducing the top storey response of the structure by using an evolutionary algorithm. They used El Centro NS earthquake to develop a computer program and found a higher percentage of reduction on the roof of a ten storey structure using TMD with the application of EVOP.

Meaghan (2013) experimentally investigated the efficiency and the parameter test on a passive auto-tuning mass damper. The results of the 'PATMD efficiency tests' demonstrate its capability of providing significant control to translational, torsional and coupled vibrations of the structure without being tuned in any way. Furthermore, the parameter study demonstrates the PATMD's effectiveness under very different conditions of the system, without having undergone any tuning or specific adjustment. The tests reveal that the PATMD is robust, uncomplicated and versatile making it an ideal application for engineering structures.

Padmabati (2015) developed a model of one-storey and a two-storey building frame for shake table experiment under sinusoidal excitation to observe the response of the structure with and without TMD. The TMD is tuned to the structural frequency of the structure keeping the stiffness and damping constant. Various parameters such as frequency ratio, mass

ratio, tuning ratio etc. are considered to observe the effectiveness and robustness of the TMD in terms of percentage reduction in amplitude of the structure. Then the responses obtained are validated numerically using finite element method. From the study it is observed that, TMD can be effectively used for vibration control of structures.

# Chapter 3.

# EXPERIMENTAL METHODS.

## 3.1. Introduction.

Tuned mass dampers are low cost seismic protection technique which are widely successful in many tall buildings and towers around the world. However they possess two main short-falls, their sensitivity to detuning and their lack of efficiency in controlling torsional and coupled vibration (translational as well as torsional).Thus till now various research works have been conducted to discover the effect of TMD to reduce the seismic shaking of the structure numerically. But experimental works under this field is quite limited. For this reason, a passive auto-tuning compound pendulum mass damper (PATCPMD) is proposed, which aims to eliminate these shortcomings.

During the experimental studies three different types of tests were carried out. The first set of tests, the PATCPMD efficiency tests, aimed at evaluating the PATCPMD's effectiveness at controlling vibration and attenuating the response of the test structure by suspending it at the second and first story of the primary model. Its efficiency in controlling transitional vibration as well as torsional and coupled vibration was under investigation. Once the PATCPMD proved to be effective, by taking the better effect from first and second story efficiency tests, a parameter test is carried out in order to evaluate its robustness against detuning. Finally the PATCPMD was suspended to the test structure in three different patterns in order to determine its efficiency under different connecting conditions. It is therefore tested under different conditions without 'tuning' the PATCPMD in any way. The natural frequencies of the primary test model is altered by changing the stiffness or the mass of the test structure.

For this experiment, free and forced vibration test is conducted to study the dynamic behaviour of a two stories frame model structure with and without PATCPMD. The structure is rigidly attached to the table platform only and the table platform in turns rigidly mounted on machine vice in case of free vibration. The structure is rigidly attached to the shaking table platform in case of forced vibration where it is subjected to sinusoidal ground motion. The fundamental frequencies of the structure is determined from free vibration analysis.

Forced vibration analysis is carried out by exciting the frame by a single frequency where as the free vibration is performed by providing some initial displacement at the top story and the response is recorded. Signal study is usually divided into time and frequency domains; each domain gives a different outlook and insight into the nature of the vibration. Time domain analysis starts by analysing the signal as a function of time. To develop the signal Ardu-

ino uno board along with Gyro accelerometer is used. The time history of acceleration analysis plots give information that helps describe the behaviour of the structure.

Frequency analysis also provides valuable information about structural vibration. Any time history signal can be transformed into the frequency domain. The most common mathematical technique for transforming time signals into the frequency domain is called the Fourier Transform. In structural analysis, usually time waveforms are measured and their Fourier Transforms are computed. The Fast Fourier Transform (FFT) is a computationally optimized version of the Fourier Transform which is used to transform time signal in to frequency domain using MATLAB R2019a.

## 3.2. Experimental Structure and Setup.

### 3.2.1. Experimental Setup.

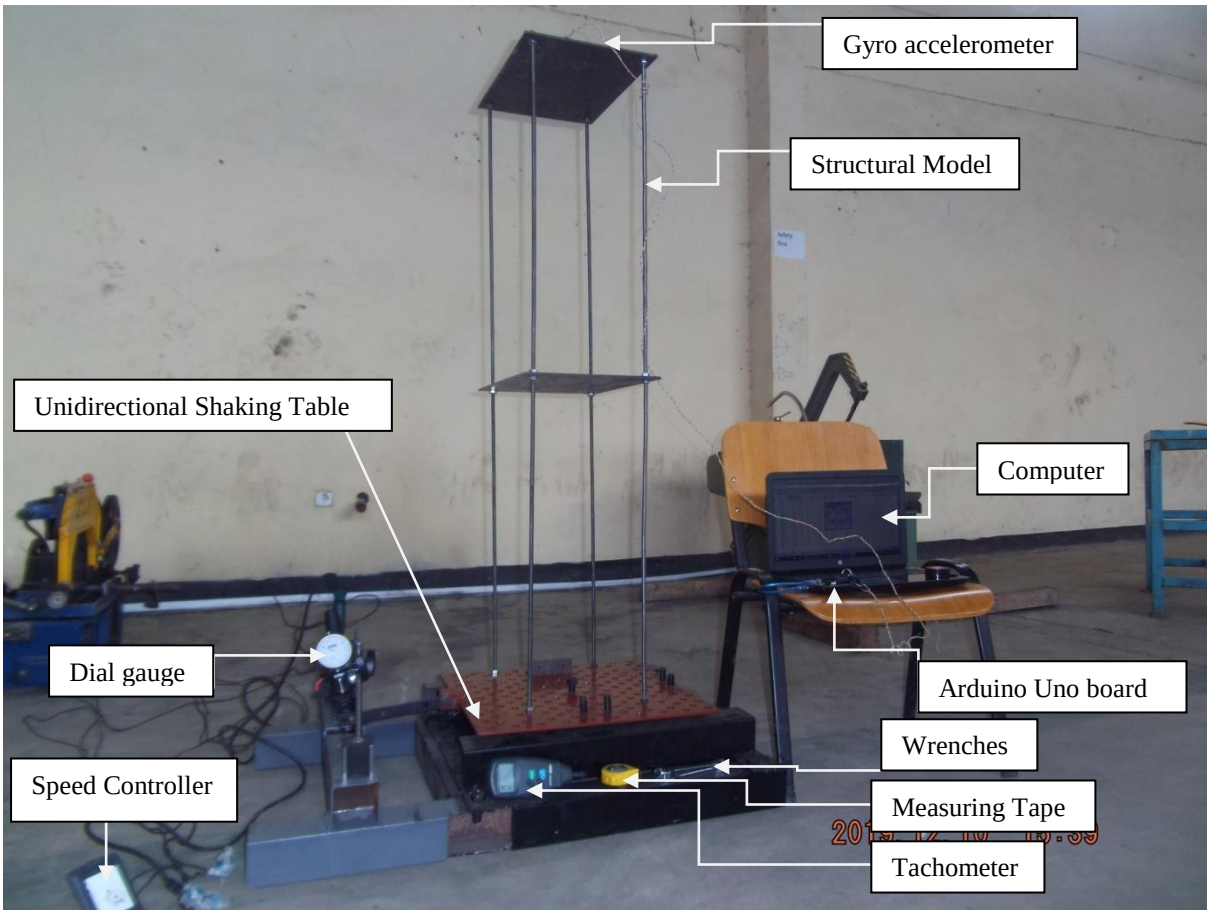


Figure 3.1. Experimental setup

The laboratory equipment consists of,

i. A unidirectional shaking table.
ii. Arduino uno board.

iii. Speed controller.
iv. Gyro accelerometer.
v. Tachometer.
vi. Measuring Tape.
vii. Dial gauge.
viii. Wrenches.
ix. Computer loaded with Arduino, PLX-DAQ and MATLAB R2019a softwares.
x. Structure Model.

#### 3.2.1.1. Unidirectional Shaking Table.

The unidirectional shaking table is made up of 0.5mx0.5m sliding plate of thickness 6mm as a platform and two mild steel round bars shafts are fixed under the plate for rotating the four aluminium rollers in a manner that the shaking table translate in one direction. The four aluminium rollers carrying the sliding plate roll on rail housing. The rail housing is fixed on to the base using bolts. And finally the base is fixed on to the ground. The translational motion is produced by using Hammer drilling machine together with crank mechanism. The drilling machine is mounted on the base perpendicular to the direction of the sliding plate motion.

The Hammer drilling machine is driven by power supply. The sliding surface has 81 drilled holes located on a 25x25mm grid for holding the model. The shake table can operate frequencies ranging from 0 to 6Hz which can be controlled by Speed controller and Tachometer. It has the capacity to produce simple harmonic motion. The maximum displacement of the table is 20 mm (± 5mm). The maximum payload of the shake table is 49.023 kg.

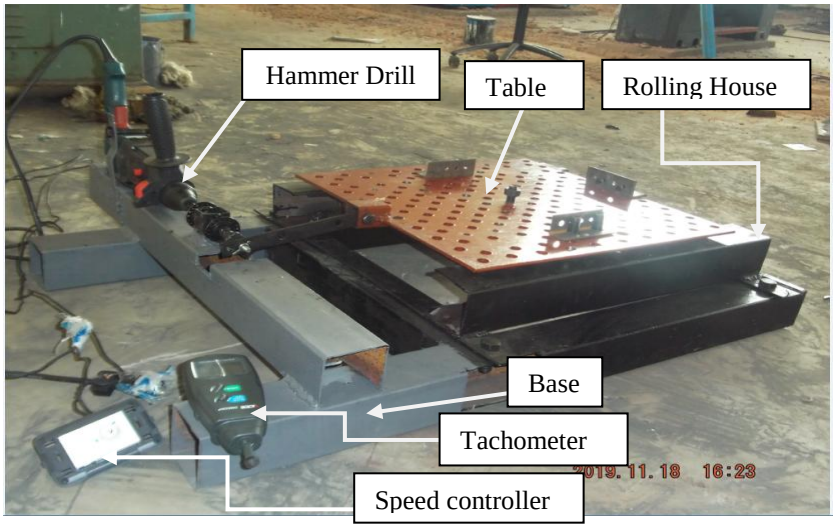


Figure 3.2. The Shaking table.

#### 3.2.1.2. Gyro Accelerometer and Arduino Uno Board.

A Gyro accelerometer is attached to the frame at the location where the acceleration needs to be measured after excitation. The Gyro accelerometer with four data cables are connected to an Arduino uno board which records the acceleration and rotation readings over time. The Arduino uno in turn is connected to a computer by USB cable so that the data acquired during the test is viewed. In order to import the data from Arduino uno serial monitor to excel format a PLX-DAQ software is used. And finally the data is analysed and processed using the MATLAB R2019a which is the most common software to perform FFT (Fast Fourier Transformer) analysis to convert the data in time domain to the frequency domain form. Thus it provides a fast, easy and accurate way to use time and frequency domain measurements for structural tests. The Gyro accelerometer and Arduino Uno board are available on Appendix B.

#### 3.2.1.3. Speed Controller.

The speed controller is managed by an input voltage of 220 volts. It is just made up of dimmer switch to control the speed of the Hammer drill machine. The revolution per minute of the drilling machine is controlled by Tachometer. It can control the excitation frequency of the shake table ranging from 0- 6Hz. The speed controller is available on Appendix B.

#### 3.2.1.4. Measuring Tape, Wrenches, Dial gauge and Tachometer.

The Measuring tape is used to measure the height of the model during height adjustment and the perpendicular height of the PATCPMD when suspended in to the plates. While Wrenches are used to loosen and tighten the nuts during height adjustment. The Dial gauge is used to check the initial displacement during free vibration test. The Tachometer is used to measure the speed of the Hammer drill which in turns control the oscillation of the shaking table in revolution per second. The Dial gauge and Tachometer photos are available on Appendix B.

#### 3.2.1.5. Structure Model.

- Material= Mild steel (both the rod and the plate)
- Unit weight of the steel=7850 kg/$m^3$
- Weight of the top plate=5.587Kg
- Weight of the bottom plate=5.692Kg
- Overall height of column = 1.38m

- Story height of column = 0.69m
- Diameter of column (D)= 9mm
- Fundamental frequency of frame (f) = 3.359 Hz, 3.42 Hz and 6.648 Hz for X-axis, Y-axis and torsional respectively. (obtained from free vibration analysis)

### 3.2.2. PATCPMD Efficiency Test.

Experimental tests were carried out on a tall, flexible two story steel floor system test model. The primary model is illustrated in Figure 3(b), whilst the model containing the PATCPMD is shown in Figure 3(a). The primary model consists of four 1.38m high, 9mm diameter threaded mild steel rod as columns and two 300mmx400mmx6mm thick mild steel plates as a slab. The plates is secured at a height of 0.69m and 1.38m for the first and second story respectively using nuts. There are eight holes drilled on the each plate for the purpose of suspending the PATCPMD to the model. The first four corner holes for the first pattern, the second four middle holes for the second pattern and the whole eight holes for the third pattern. And the compound pendulum is manufactured using sheet metal and there is a hole at the top centre of the compound pendulum in order to suspend the mass damper and there are eight holes on the compound pendulum base so as to suspend the whole pendulum on to the floors of the model as per their pattern. Inelastic string is used to suspend the compound pendulum and the mass damper. The columns are bolted rigidly to a unidirectional shaking table platform such that the ends are rotationally fixed. ETABS 2016 Structural software is used to simulate the behaviour of the primary model, and to determine its first three natural frequencies and associated mode shapes. As far as possible the values of the dynamic properties of the primary model that is obtained from the Structural software simulation is made to closely matches those which would be expected for a real-life tall, flexible structure. A number of model dimensions were entered and simulated until suitable frequency values were obtained, and therefore suitable model dimensions were decided. The simulated model's first three natural frequencies, corresponding to the first three mode shapes are $f_1$=3.359Hz, $f_2$= 3.42Hz and $f_3$=6.648Hz as shown in Figure 4. The aspect ratio of the model is perhaps not very similar to that of a real life structure, however the aspect ratio is not a critical property at this stage as the principle of the PATCPMD is under investigation in this report. The model with PATCPMD is suspended at the first and second story shown in Appendix B.

The PATCPMD, shown attached to the primary model in Figure 3(a) and the close up photo on Appendix B, is manufactured in the form of compound pendulum but not exactly where the link is made up of galvanized sheet metal of mass 0.457kg and the damper made up of

aluminium of mass 0.153kg. Then it has a whole mass of 0.611kg which is about 4% of the primary model's mass of 14.104kg. It is suspended, with inelastic ropes, to the eight holes at a perpendicular height of 70mm below the plates and the damper mass in turns suspended in the middle centre of the link at a height of 40mm. The rope was used in the experiments due to its inelastic and flexible nature.

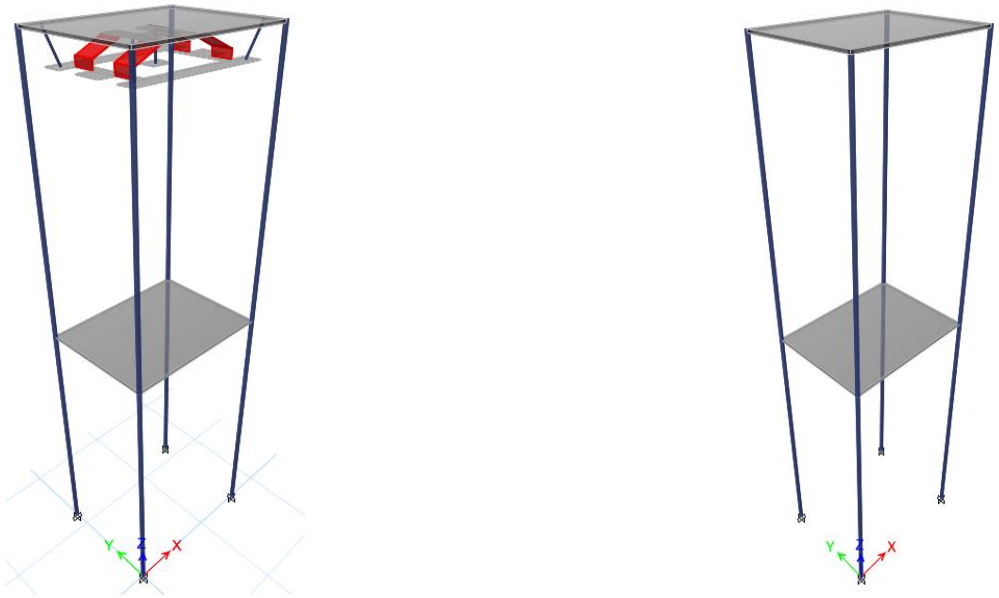

Figure 3.3. (a) The test model containing the PATCPMD. (b) The primary test model.

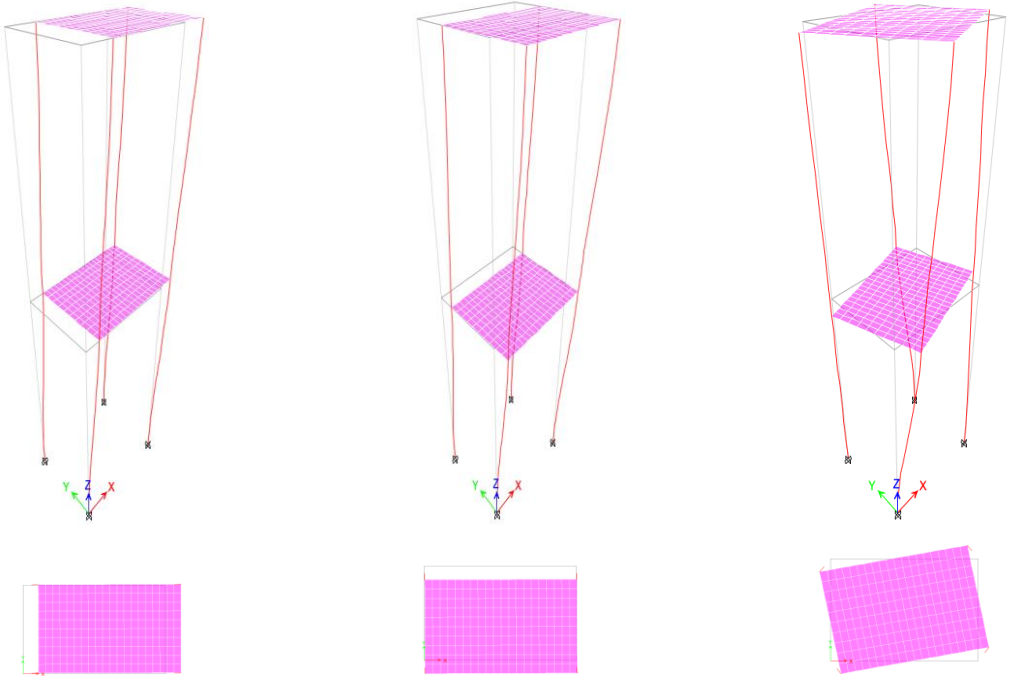

Mode 1: Translation in the X-direction $f_1$=3.359Hz.

Mode 2: Translation in the Y-direction $f_2$=3.42Hz

Mode 3: Torsion. $f_3$=6.648Hz

Figure 3.4.The primary model's first three natural frequencies and corrosponding modal shapes.

### 3.2.3. Changing The Model's Stiffness.

The stiffness of the test model was changed by altering its height. The steel plates were moved down as needed and were secured to the threaded rod columns at various heights using nuts. The model was set to heights of 1.38m with equal story height of 0.69m, 1.2m with equal story height of 0.6m and 1m with equal story heights of 0.5m for the tests. The PATCPMD was not adjusted at all during these tests, the mass ratio was kept constant and the connection to the test model remained unchanged during the tests. Again, ETABS 2016 Structural software simulation was carried out in order to check the natural frequencies which could be expected in the experimental tests, prior to carrying them out. Figure 5. shows the three ETABS 2016 models considered in the simulations, which are presented in Appendix A.

| 1m with equal story heights of 0.5m Model. | 1.2m with equal story heights of 0.6m Model. | 1.38m with equal story heights of 0.69m Model. |
|---|---|---|
| 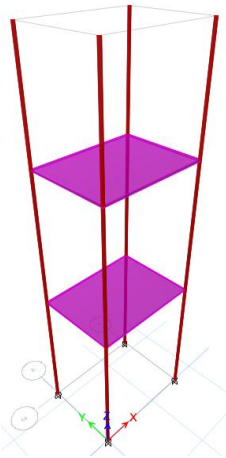 | 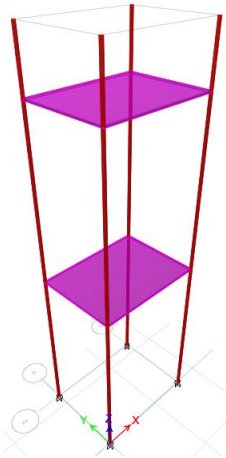 | 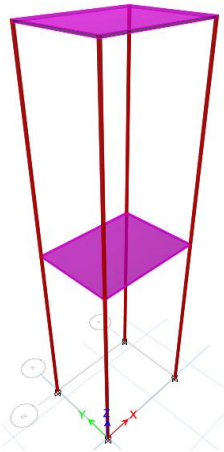 |
| Mode 1: Translation in the X-direction, $f_1$=5.035Hz. | Mode 1: Translation in the X-direction, $f_1$=4.011Hz. | Mode 1: Translation in the X-direction, $f_1$=3.359Hz. |
| Mode 2: Translation in the Y-direction, $f_2$=5.15Hz. | Mode 2: Translation in the Y-direction, $f_2$=4.091Hz. | Mode 2: Translation in the Y-direction, $f_2$=3.42Hz. |
| Mode 3: Torsion, $f_3$=8.701Hz. | Mode 3: Torsion, $f_3$=7.47Hz. | Mode 3: Torsion, $f_3$=6.648Hz. |

Figure 3.5. A ETABS 2016 illustration of the three heights at which the model was tested so as to vary the model's stiffness- 0.5m, 0.6m and 0.69m equal story height respectively.


(a) (b) (c)

Figure 3.6. Photographs of the three heights at which the model was tested in order to change the model's stiffness- 0.5m, 0.6m and 0.69m equal story height respectively.

### 3.2.4. Changing The Model's Mass.

Next, the mass of the test model was varied whilst its height was kept constant at 1.38m with equal story height of 0.69m. The PATCPMD was not adjusted during the tests; its mass was kept constant at 0.611kg. The primary test structure's mass was 14.104kg, and extra weights of 0.298kg were secured to each primary steel plates so that the mass of 14.7kg was achieved. These two model masses, shown in Figure 8. were considered for testing.

Again, a ETABS 2016 Structural Software simulation was carried out in order to check the natural frequencies which could be expected in the experimental tests, prior to carrying them out. In ETABS 2016, a thicker steel plates were considered in order to reach the required model masses. Figure 7. shows the two ETABS 2016 models considered in the simulations, which are presented in Appendix A.

Model Mass 14.104kg.

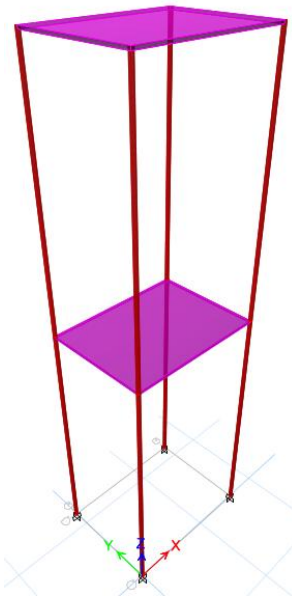

Mode 1: Translation in the X-direction, $f_1$=3.359Hz.

Mode 2: Translation in the Y-direction, $f_2$=3.42Hz.

Mode 3: Torsion, $f_3$=6.648Hz.

Model Mass 14.7kg.

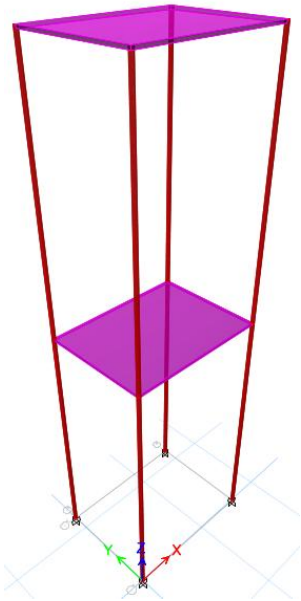

Mode 1: Translation in the X-direction, $f_1$=3.346Hz.

Mode 2: Translation in the Y-direction, $f_2$=3.401Hz.

Mode 3: Torsion, $f_3$=6.602Hz.

Figure 3.7. A ETABS 2016 illustration of the two masses at which the model was tested – 14.104kg and 14.7kg respectively.

Figure 3.8. Photographs of the two masses at which the model was tested – 14.104kg and 14.7kg respectively.

### 3.2.5. Changing the PATCPMD's Connection Pattern to the Test Model.

The PATCPMD was suspended to the test structure in three different patterns in order to determine its efficiency under different connecting conditions. The different connections are described below and are shown in ETABS 2016 models in Figure 9 and photos in Figure 10.
Pattern 1 – The four corner ropes are all suspended at an angle with the same perpendicular height of 70mm below the plate. And the mass damper in turn is suspended at the middle centre of the PATCPMD with the 40mm height.

Pattern 2 – The four side ropes are all suspended at an angle with the same perpendicular height of 70mm below the plate. And the mass damper in turn is suspended at the middle centre of the PATCPMD with the 40mm height.

Pattern 3 – The four corner ropes and the four side ropes are all suspended at an angle with the same perpendicular height i.e. 70mm below the plate. And the mass damper in turn is suspended at the middle centre of the PATCPMD with the 40mm height.

Pattern 1. Pattern 2. Pattern 3.

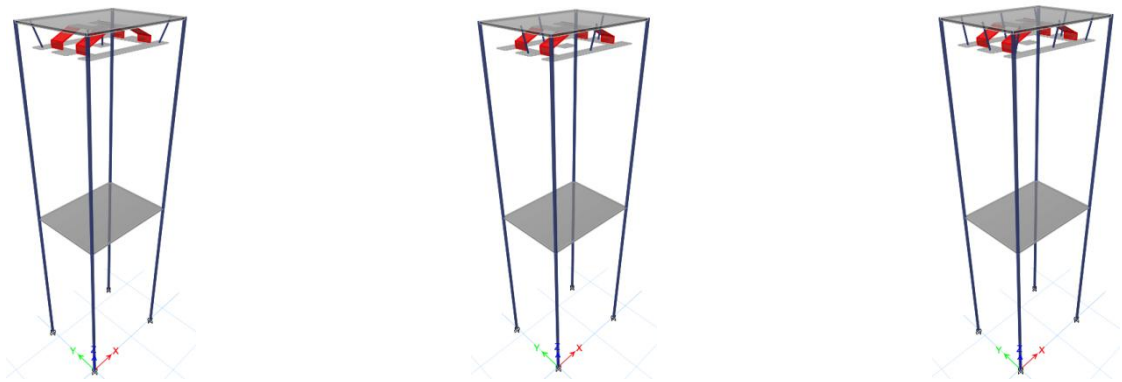

Figure 3.9. An illustration of the different PATCPMD connection patterns that were tested.

Figure 3.10. Photographs of the three patterns- Pattern 1, Pattern 2 and Pattern 3 respectively.

## 3.3. Experimental Procedure.

### 3.3.1. Free Vibration Tests.

The following testing procedure was undertaken in the PATCPMD efficiency tests, parameter tests and tests carried out to observe the effect of PATCPMD's connection on the damping of the structure. Free vibration tests were performed on the primary test model (without PATCPMD). The model was excited by giving it an initial displacement of 10mm, which was measured using a dial indicator, and then releasing it. The tests were excited in two translational directions; torsion; and lastly it was given two coupled excitations. The two translational directions were the orthogonal X and Y-directions. It was excited torsionally by applying an initial twist to the model with a translational displacement of 10mm and then releasing it. Lastly, the model was subjected to two coupled excitations which were achieved by giving it initial translational as well as torsional displacements simultaneously.

The PATCPMD was then suspended to the primary structure first at the upper story and second at the lower story and the tests described above was repeated in order to obtain the better effect. Once the better effect is obtained using the remaining tests were performed by considering the better effect. The sampling frequency chosen for these experiments was 10Hz, meaning that 10 acceleration readings were collected by the data logger per second. The Gyro accelerometer is capable of recording the acceleration readings in two directions and therefore did not have to be reorientated during the testing procedure. SSMS (Single-Sided Magnitude Spectrum) graphs, time-history of acceleration and time-history of rotation graphs were used to show the PATCPMD's damping effects at the primary model.

### 3.3.2. Forced Vibration Tests.

Forced vibration tests also carried out on the test structure with and without the PATCPMD. The test model was secured to a unidirectional shaking table which produced a sinusoidal base excitation. The stroke of the table was 20mm. The forced tests was carried out in two directions; the translational X-direction and Y-direction. No forced torsional vibration tests was carried out due to the fact that a forced torsional excitation could not be produced with this shaking table. The frequency was around 1.5Hz for all of the tests due to the fact that it was fluctuating because of the power supply. SSMS graphs was used to show the damping effects of the PATCPMD.

# Chapter 4.

# EXPERIMENTAL TESTS.

## 4.1. Introduction.

In the Experimental tests four different types of tests were undertaken. The first set of tests were the PATCPMD efficiency tests where the PATCPMD was suspended first at the upper story and second at the lower story in order to know the better effect. Once the better effect of the PATCPMD was obtained the remaining three set of tests were carried out by suspending the PATCPMD at the story where better effect was found. In order to demonstrate the auto-tuning properties of the proposed PATCPMD, the dynamic properties, such as the natural frequencies of the test structure, the second and third set of tests were carried out by changing the model's stiffness and mass. Changing the model's stiffness is achieved by changing the length of the columns from 0.69m equal story height to 0.6m and 0.5m equal story height where as changing the model's mass is achieved by adding 0.298kg equal masses to the test structure on the first and the second stories. In all cases no tuning or adjustment of the PATCPMD took place. In the last set of tests the PATCPMD was connected to the primary structure in three different patterns in order to determine the effect of this connection on the damping of the structure. During these tests, no adjustment of the PATCPMD's mass ratio took place; and the mass and stiffness of the primary structure were left constant at 14.104kg and 1.38m overall high respectively. The three different patterns have been described and shown in photographs in Section 3.2.5.

## 4.2. PATCPMD Efficiency Tests at the First and Second Story.

### 4.2.1. Free Vibration.

#### 4.2.1.1. Translational Vibration in the X-Direction.

An initial displacement of 10mm was given to the primary test model at the top story in the X-direction before releasing it. The PATCPMD was then suspended first in the upper story and second in the lower story and this procedure was repeated. The Gyro accelerometer is attached to the top story to read the acceleration in the X direction. The Single-Sided Magnitude Spectrum (SSMS) Figure 11(b) below shows a high peak without PATCPMD at 3.0151Hz which is the model's natural frequency for translation in the X-direction. It is observed that the natural frequencies obtained by simulation (3.297Hz) and by experimentation (3.0151Hz) do not match up exactly, however they are very close in value. This is to be ex-

pected as the simulation results represent those of an 'ideal' test. Figure 11(b) shows that the PATCPMD provides a high level of attenuation to the peak when the PATCPMD is suspended at the second story. The peak under consideration, 3.0151Hz is reduced by 48.0% when the PATCPMD is suspended on the first story and by 79.9% when the PATCPMD is suspended on the second story. The time history of acceleration response shows that near the beginning of the test, as the PATCPMD starts moving, the acceleration peaks generated in the damped model are a little bit high when the PATCPMD is suspended on the first story, exceeding those generated in the undamped model whereas the acceleration peaks generated in the damped model are low when the PATCPMD is suspended on the second story compared to those generated in the undamped model. These high accelerations rapidly become less specially when the PATCPMD is suspended on the second story than those found in the undamped model; however these initial high accelerations occurred when the PATCPMD is suspended in the first story are undesirable. Regardless of this small modification, the positive damping effects of the PATCPMD evident in Figures 11(a) and Figure 11(b) are still significant .

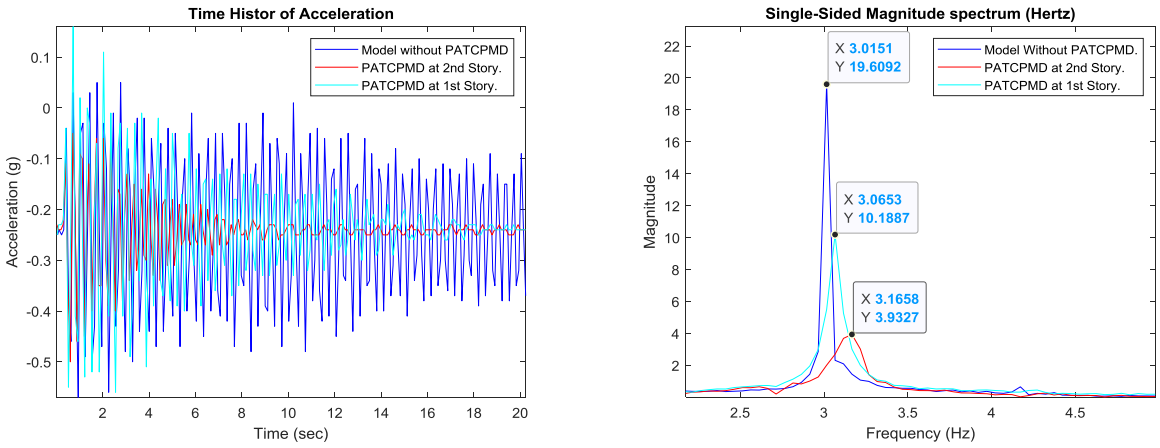


(a) (b)

Figure 4.1. For free translational vibration in the X-direction (a) Time history of acceleration response (b) Single-sided magnitude spectrum (SSMS) of the acceleration response.

#### 4.2.1.2. Translational Vibration in the Y-Direction.

Next, An initial displacement of 10mm was given to the primary test model at the top story in the Y-direction before releasing it. The PATCPMD was then suspended first in the second story and second in the first story and this procedure was repeated. The Gyro accelerometer is attached to the top story to read the acceleration in the Y direction. The SSMS graph shows a

high peak at 3.1156Hz, which is the model's natural frequency in the Y-direction. Again, this is very similar to the simulated result of 3.355Hz. The peak is reduced significantly as the structure is controlled by the addition of the PATCPMD in the second and first story. The peak natural frequency for translation in the Y-direction, 3.1156Hz, is reduced by 75.4% when the PATCPMD is suspended on the first story and 88.8% when the PATCPMD is suspended on the second story. The time history of acceleration response, shown in Figure 12(a), contains almost similar acceleration peaks for the damped model initially as the PATCPMD starts moving at both when it is suspended in the first and second story, with these peaks rapidly decreasing to well below those of the undamped model specially when the PATCPMD is suspended at the second story.

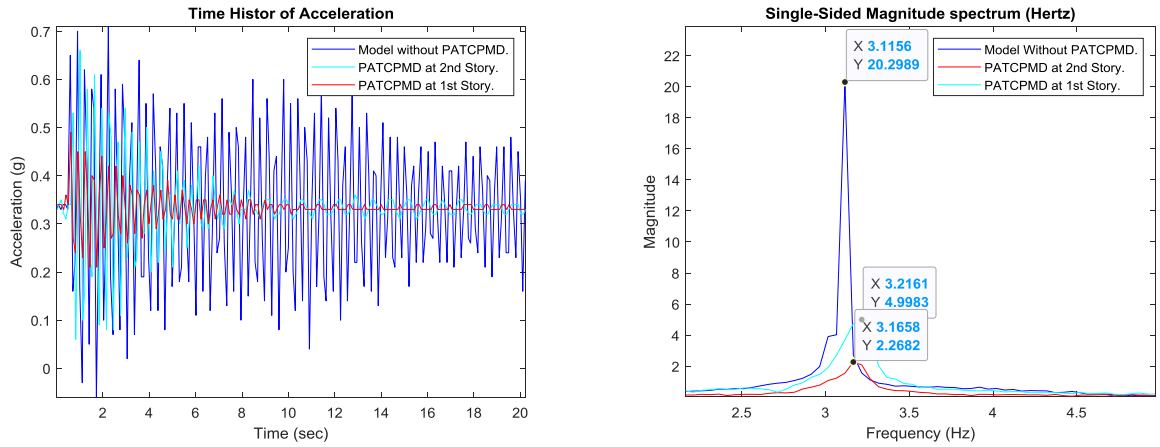


(a) (b)

Figure 4.2. For free translational vibration in the Y-direction (a) Time history of acceleration response (b) Single-sided magnitude spectrum (SSMS) of the acceleration response.

#### 4.2.1.3. **Torsional Vibration.**

Next, the primary model was displaced at the top story torsionally by a translational displacement of 10mm before releasing it. The PATCPMD was then connected first at the second story and second at the first story and this procedure was repeated. Gyro accelerometer is attached to the top story to read the rotation in degree in order to observe the effect of the PATCPMD on torsional vibration. The SSMS graph below shows a high peak at 4.0882Hz , which is the model's torsional natural frequency . It is observed that the natural frequencies obtained by simulation (6.648Hz) and by experimentation (4.0882Hz) do not match up exactly. This is to be expected as the simulation results represent those of an 'ideal' test. Once

again, the peak is reduced by the addition of the PATCPMD, with the peak at 4.0882Hz, being reduced by 64.4% when the PATCPMD is suspended at the first story and 87.3% when the PATCPMD is suspended at the second story. The time history of rotation response of the torsion for the model containing the PATCPMD shows a rapid decrease in rotations when the PATCPMD is suspended at the first story and relatively more rapid when it is suspended at the second story as opposed to the previous translational time history graphs. This shows that the effect of the PATCPMD is still obvious as time passes specially when the PATCPMD is suspended at the second story.

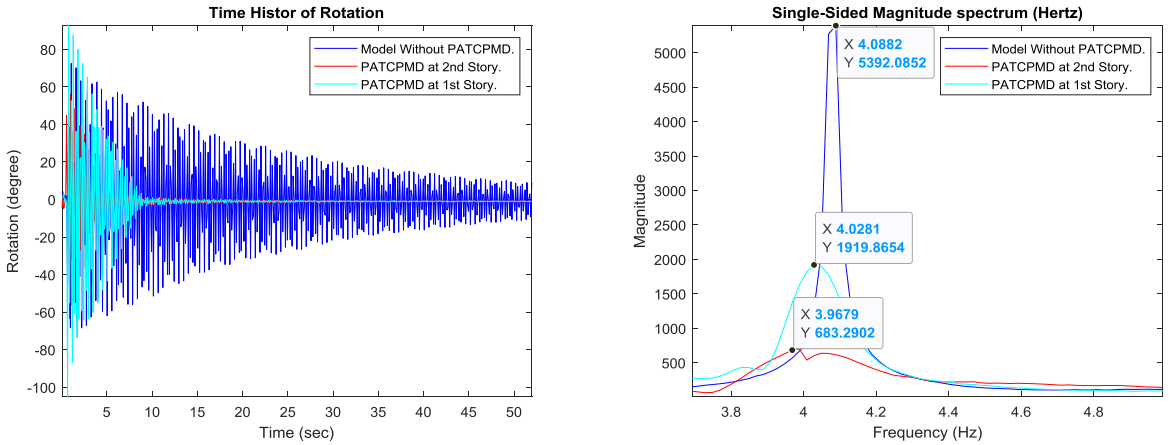


(a) (b)

Figure 4.3. For free torsional vibration (a) Time history of rotation response (b) Single-sided magnitude spectrum (SSMS) of the rotation response.

#### 4.2.1.4. Coupled Vibration (Translational in the X-Direction and Torsion)

Next, the model was subjected to a coupled excitation - it was given initial translational displacement of 10mm in the X-direction and torsional displacements of 10mm at the top story simultaneously before releasing it. The PATCPMD was then connected first at the second story and second at the first story and this procedure was repeated. Gyro accelerometer is attached to the top story to read both the rotation and acceleration in order to observe the effect of the PATCPMD on coupled vibration. The SSMS graphs below show high peaks at 4.0681Hz for the torsional natural frequency and 3.0661Hz for the transitional X direction natural frequency. The peaks are reduced by the addition of the PATCPMD by 65.9% when the PATCPMD is suspended at the first story and 75.4% when the PATCPMD is suspended at the second story for torsion and by 53.5% when the PATCPMD is suspended at the first

story and 84.9% when the PATCPMD is suspended at the second story for translation in the X direction. The time history of rotation and acceleration response shows that near the beginning of the test, as the PATCPMD starts moving, the acceleration and rotation peaks generated in the damped model are a little bit high. However, the effect of the PATCPMD is still obvious as time passes specially when the PATCPMD is suspended at the second story.

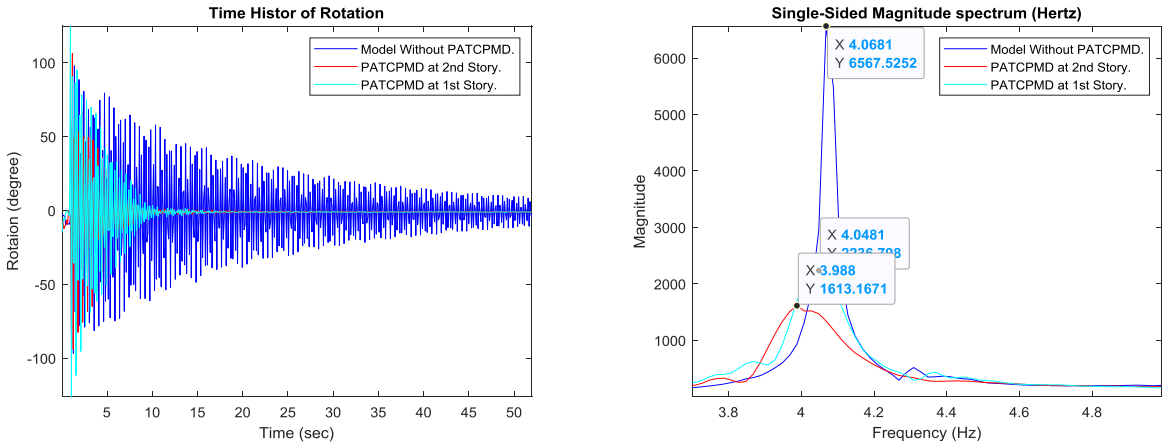


(a) (b)

Figure 4.4. For free coupled ( torsional and X axis) torsional vibration (a) Time history of rotation response (b) Single-sided magnitude spectrum (SSMS) of the rotation response.

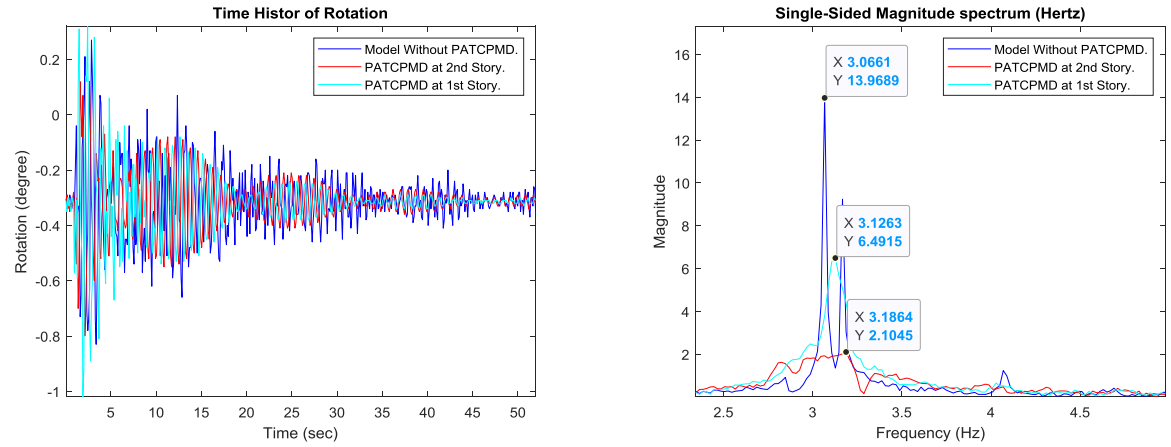


(a) (b)

Figure 4.5. For free coupled (torsion and X axis) translational X axis vibration (a) Time history of acceleration response (b) Single-sided magnitude spectrum (SSMS) of the acceleration response.

#### 4.2.1.5. Coupled Vibration (Translation in the Y-Direction and Torsion)

Lastly, the model was subjected to a coupled excitation - it was given initial translational displacement of 10mm in the Y-direction and torsional displacements of 10mm at the top story at the same time before releasing it. The PATCPMD was then connected first at the second story and second at the first story and this procedure was repeated. Gyro accelerometer is attached to the top story to read both the rotation and acceleration in order to observe the effect of the PATCPMD on coupled vibration. The SSMS graphs below show high peaks at 4.0882Hz for the torsional natural frequency and 3.0661Hz for the transitional Y direction natural frequency. The peaks are reduced by the addition of the PATCPMD by 66.3% when the PATCPMD is suspended at the first story and 80.9% when the PATCPMD is suspended at the second story for torsion and by 75.4% when the PATCPMD is suspended at the first story and 90.0% when the PATCPMD is suspended at the second story for translation in the Y direction . The time history of rotation and acceleration response show that near the beginning of the test, as the PATCPMD starts moving, the acceleration and rotation peaks generated in the damped model are also a little bit high. However, the effect of the PATCPMD is still obvious as time passes specially when the PATCPMD is suspended at the second story.

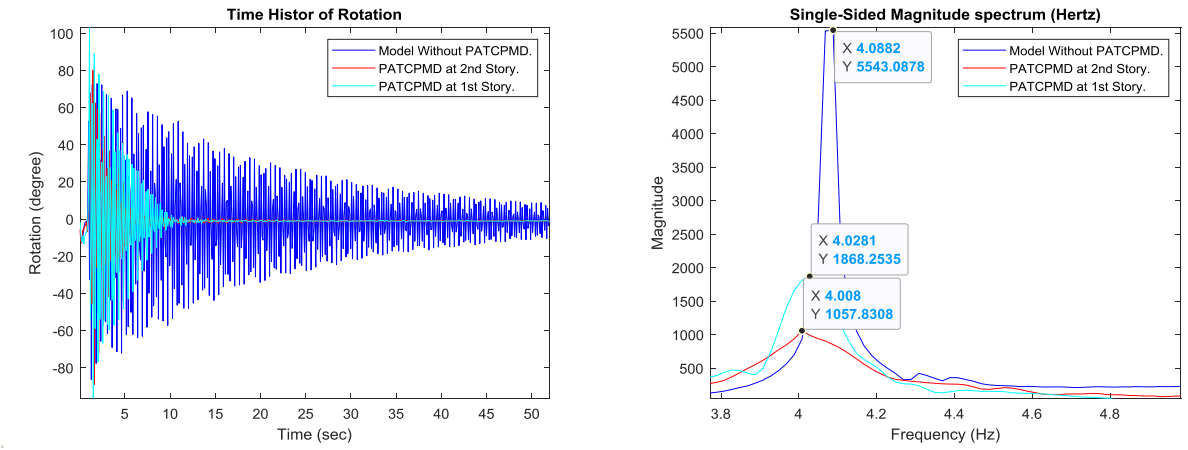


(a) (b)

Figure 4.6. For free coupled ( torsional and Y axis ) torsional vibration (a) Time history of rotation response (b) Single-sided magnitude spectrum (SSMS) of the rotation response.

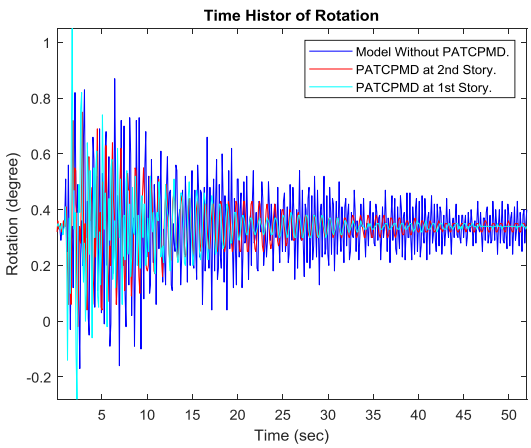


(a)

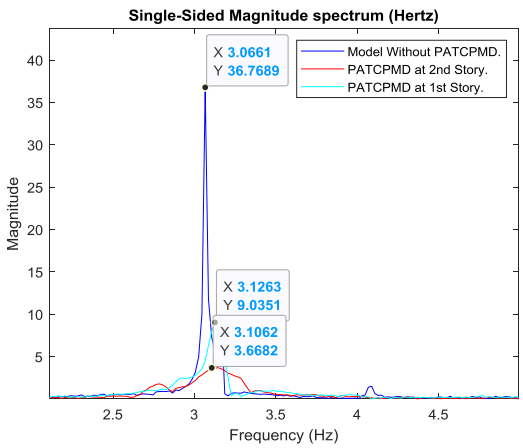


(b)

Figure 4.7. For free coupled (torsion and Y axis) translational Y axis vibration (a) Time history of acceleration response (b) Single-sided magnitude spectrum (SSMS) of the acceleration response.

### 4.2.2. Forced Vibration.

#### 4.2.2.1. Translational Vibration in the X-Direction.

First, the test model was orientated on the shaking table so as to generate forced vibrations in the X-direction on the model. The SSMS peak is seen at 1.2375Hz. The control provided by the PATCPMD during the forced vibration tests is obvious from the SSMS graph in Figure 18, where the peak occurring at the natural frequency for translational vibration in the X-direction is reduced by 88.5% and 68.4% when the PATCPMD is suspended at the second and first story respectively.

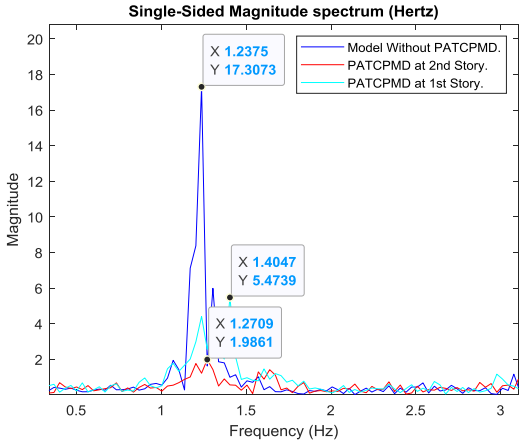


Figure 4.8. Single-sided magnitude spectrum (SSMS) of the acceleration response for forced translational vibration in the X direction.

#### 4.2.2.2. Translational Vibration in the Y-Direction.

The test model was then turned 90° on the shaking table so as to experience forced vibrations in the Y-direction. The SSMS peak is seen at 1.2709Hz. The control provided by the PATCPMD during the forced vibration tests is obvious from the SSMS graph in Figure 19, where the peak occurring at the natural frequency for translational vibration in the Y-direction is reduced by 81.3% and 13.0% when the PATCPMD is suspended at the second and first story respectively.

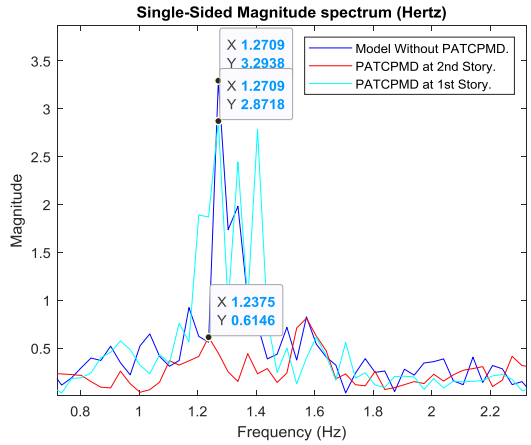


Figure 4.9. Single-sided magnitude spectrum (SSMS) of the acceleration response for forced translational vibration in the Y direction.

### 4.2.3. Summary and Conclusion.

The experimental test results above reveal that the PATCPMD can successfully attenuate translational, torsional and coupled vibration when the PATCPMD is suspended both in the first and second story and subjected to free or forced excitations. The SSMS peak was reduced by between 13.0%-75.4% for translational vibrations and 64.4%-66.3% for torsional vibrations when the PATCPMD is suspended in the first story and by between 79.9%-90.0% for translational vibrations and 75.4%-87.3% for torsional vibrations when the PATCPMD is suspended in the second story which demonstrates its ability to effectively control all three types of excitation. However, as can be observed from the results, the better attenuation of the vibration control is observed when the PATCPMD is suspended on the second story. This is a vast advantage over TMDs which can, in general, only control a single frequency. Furthermore, torsional vibration, which has been more difficult to control, was significantly attenuated. Hence here after the parameter tests and tests carried out to observe the effect of PATCPMD's connection on the damping of the structure are performed

by suspending the PATCPMD at the second story since better effect is achieved on the second story.

## 4.3. Effects of Changing Model's Stiffness.

### 4.3.1. Free Vibration.

#### 4.3.1.1. Translational Vibration in the X-Direction.

The SSMS and time history of acceleration graphs for models of different stiffness, subjected to translational vibration in the X direction, are shown below. The mass ratio was kept constant at 4% during the tests that follow. The stiffness of the model increases significantly with decreased model height, therefore, the natural frequencies also change considerably. As is to be expected, the model with 0.5m equal story height has the greatest stiffness, whilst the 0.69m equal story height model is the least stiff for vibration in all directions. The experimental value for natural frequency obtained from the tests for the 0.5m equal story heights model is 4.6924Hz, for the 0.6m equal story heights model is 3.6767Hz and for the 0.69m equal story heights model is 3.0151Hz, which are similar to the simulated results 5.035Hz, 4.011Hz and 3.359Hz respectively as shown earlier. In all cases, the model containing the PATCPMD has a smaller peak SSMS reading than the model without the PATCPMD. The SSMS peaks were reduced by 53.8%, 80.4% and 79.8% for 0.5m, 0.6m and 0.69m equal story heights respectively by the addition of the PATCPMD. The time-history of acceleration graphs show that near the beginning of the test, as the PATCPMD starts moving, the acceleration peaks generated in the damped model are low, less than those generated in the undamped model followed by a rapid decrease in all the cases. The positive damping effects of the PATCPMD are still significant. These graphs demonstrate that even though the natural frequencies of the test structure were changed by changing the story height of the model, the PATCPMD, without any tuning or adjustment, produced effective control on the X-direction translational vibration for each case.

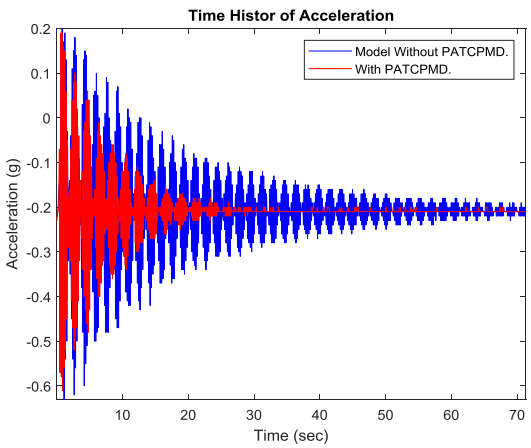


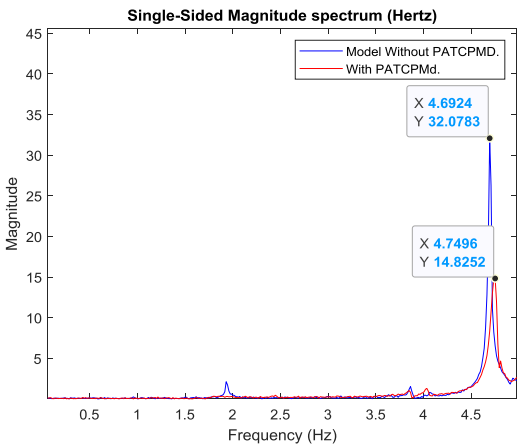


(a) (b)

Figure 4.10. For free translational vibration in the X direction for model equal height of 0.5m (a) Time history of acceleration response (b) Single-sided magnitude spectrum (SSMS) of the acceleration response.

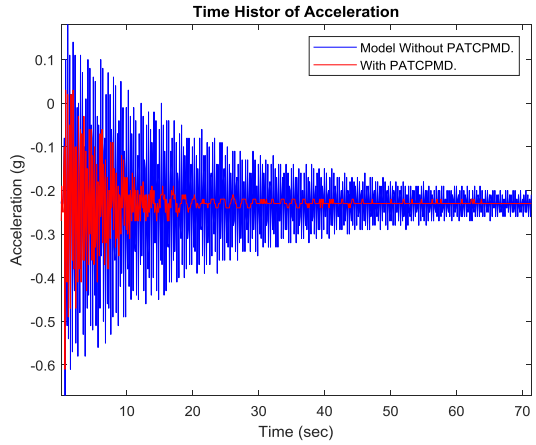


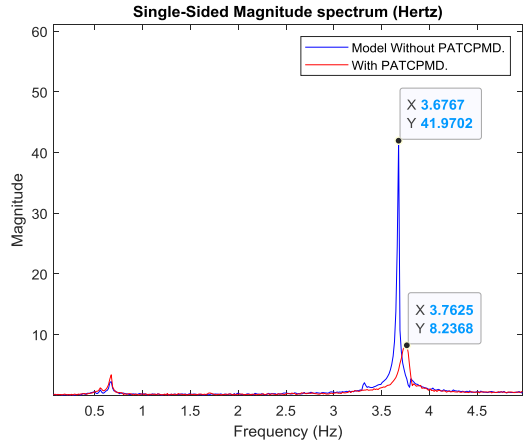


(a) (b)

Figure 4.11. For free translational vibration in the X direction for model equal height of 0.6m (a) Time history of acceleration response (b) Single-sided magnitude spectrum (SSMS) of the acceleration response.

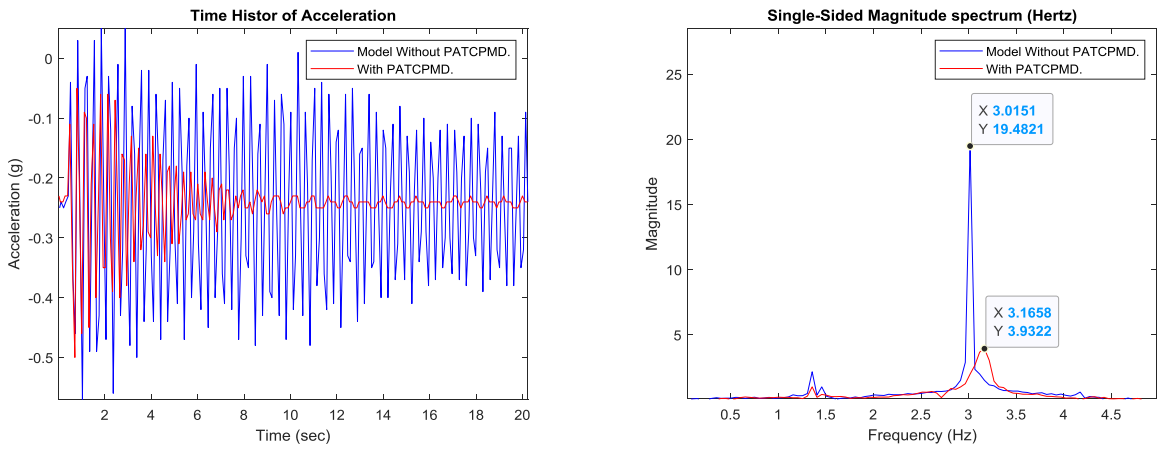


(a) (b)

Figure 4.12. For free translational vibration in the X direction for model equal height of 0.69m (a) Time history of acceleration response (b) Single-sided magnitude spectrum (SSMS) of the acceleration response.

#### 4.3.1.2. Translational Vibration in the Y-Direction.

The SSMS and time-history of acceleration graphs for models of different stiffness, subjected to translational vibration in the Y direction, are shown below. The natural frequencies change significantly as the model stiffness is altered. The experimental value for natural frequency obtained from the tests for the 0.5m equal story heights model is 4.9246Hz, for the 0.6m equal story heights model is 3.8054Hz and for the 0.69m equal story heights model is 3.1156Hz, which are in close agreement with the simulated results 5.15Hz, 4.091Hz and 3.42Hz respectively as shown earlier. In all cases, the model with the PATCPMD, has a smaller peak SSMS reading. The SSMS peaks were reduced by 51.4%, 49.4% and 75.4% for 0.5m, 0.6m and 0.69m equal story heights respectively by the addition of the PATCPMD. Again, the time-history of acceleration graphs show that near the beginning of the test, as the PATCPMD starts moving, the acceleration peaks generated in the damped model are very high on model with 0.5m and 0.6m equal story height, exceeding those generated in the un-damped model. However, regardless of this small modification, the positive damping effects of the PATCPMD are still significant. This demonstrates that the PATCPMD, without any tuning or adjustment, can produce effective control on the Y-direction translational vibration even when the natural frequencies of the test structure are changed.

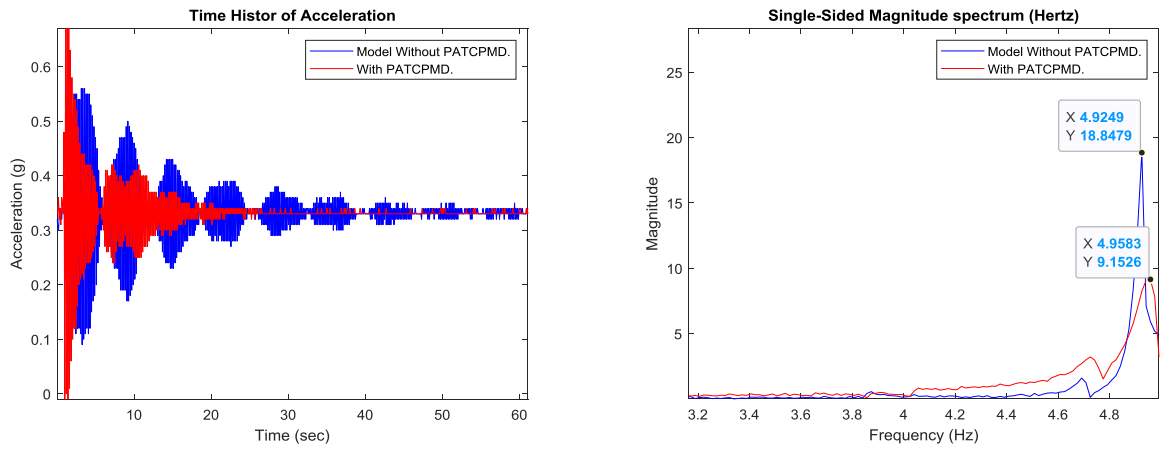


(a) (b)

Figure 4.13. For free translational vibration in the Y direction for model equal height of 0.5m (a) Time history of acceleration response (b) Single-sided magnitude spectrum (SSMS) of the acceleration response.

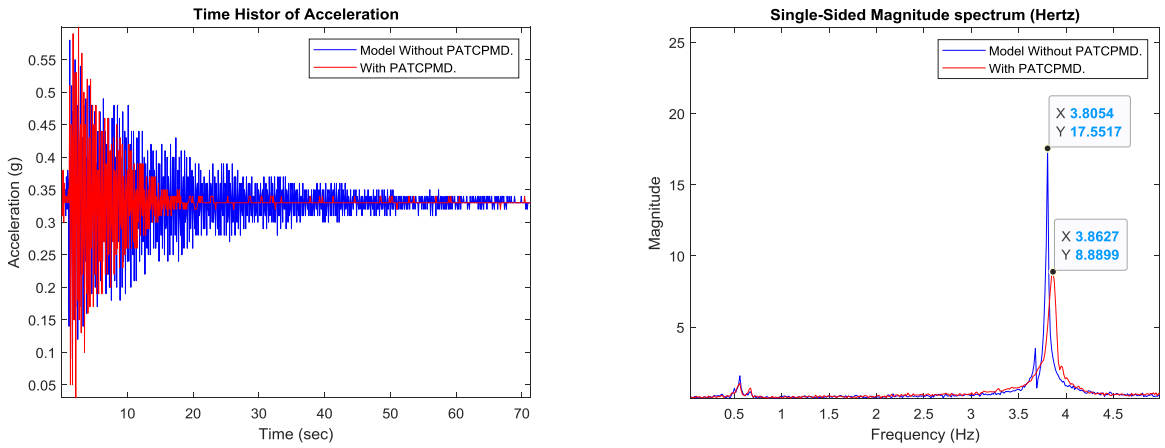


(a) (b)

Figure 4.14. For free translational vibration in the Y direction for model equal height of 0.6m (a) Time history of acceleration response (b) Single-sided magnitude spectrum (SSMS) of the acceleration response.

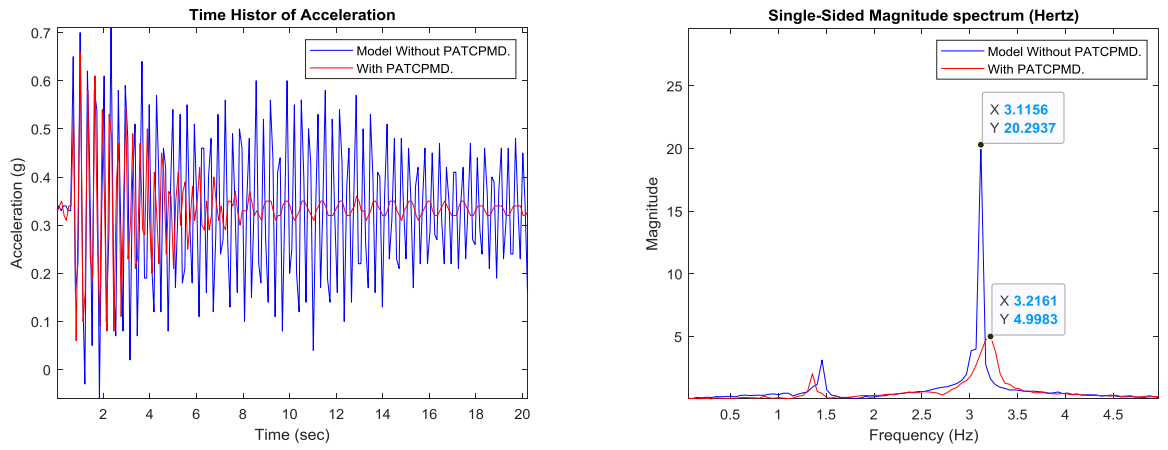


(a) (b)

Figure 4.15. For free translational vibration in the Y direction for model equal height of 0.69m (a) Time history of acceleration response (b) Single-sided magnitude spectrum (SSMS) of the acceleration response.

#### 4.3.1.3. **Torsional Vibration.**

The SSMS and time-history graphs for models of different stiffness, subjected to torsional vibration are shown below. As can be seen in Figure 26(b), Figure 27(b) and Figure 28(b) below, the natural frequencies for torsion also change significantly with changing model stiffness. It is observed that the natural frequency of the model obtained from simulation results for the 0.5m equal story height model is 8.701Hz, for the 0.6m equal story height model is 7.47Hz and for the 0.69m equal story height model is 6.648Hz and by experimentation 1.8445Hz, 3.2401Hz and 4.0773Hz respectively do not match up exactly. This is to be expected as the simulation results represent those of an 'ideal' test. As expected, these frequencies are higher than the frequencies for translational vibration due to the model's increased stiffness in torsion. In all cases, the model with the PATCPMD, has a smaller peak SSMS reading. The SSMS peaks were reduced by 78.3%, 51.3% and 91.8% for 0.5m, 0.6m and 0.69m equal story heights respectively by the addition of the PATCPMD. Again, the time history graphs show that near the beginning of the test, as the PATCPMD starts moving, the rotation peaks generated in the damped model are a little bit high on model with 0.6m equal story height, exceeding those generated in the undamped model. However, regardless of this small modification, the positive damping effects of the PATCPMD are still significant. This demonstrates that the PATCPMD, without any tuning or adjustment, can produce effective control on the torsional vibration even when the natural frequencies of the test structure are changed.

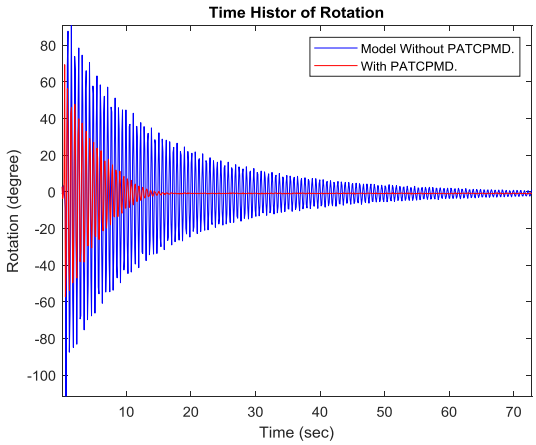


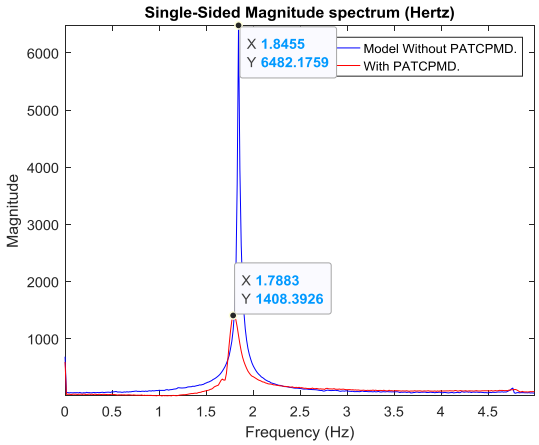


(a) (b)

Figure 4.16. For free torsional vibration model with equal story height of 0.5m (a) Time history of rotation response (b) Single-sided magnitude spectrum (SSMS) of the rotation response.

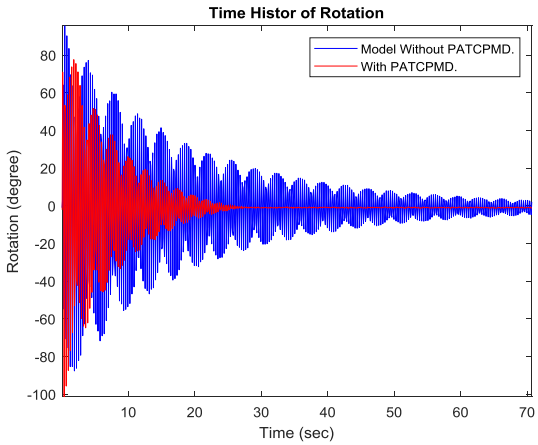


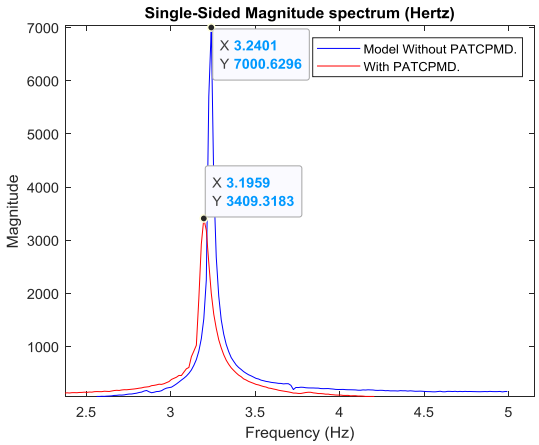


(a) (b)

Figure 4.17. For free torsional vibration model with equal story height of 0.6m (a) Time history of rotation response (b) Single-sided magnitude spectrum (SSMS) of the rotation response.

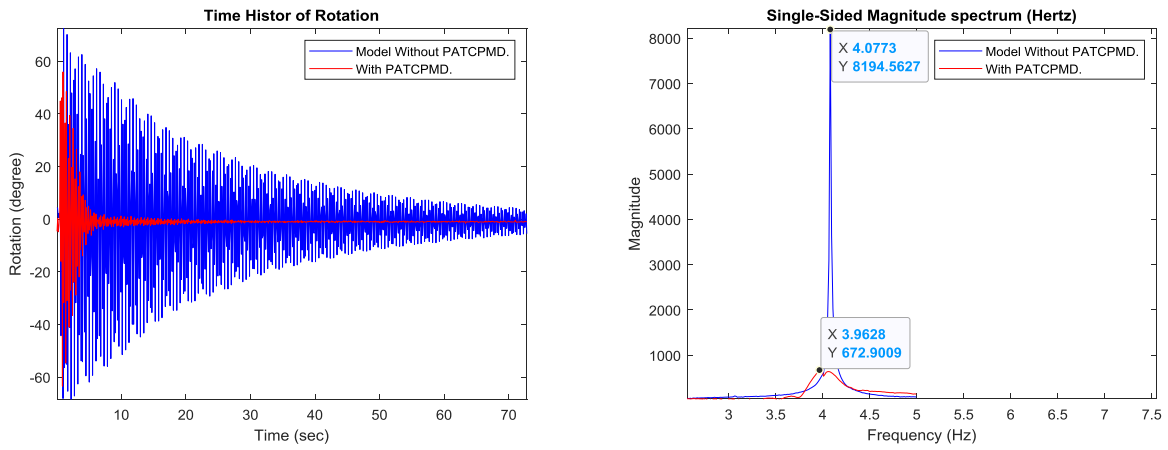


(a) (b)

Figure 4.18. For free torsional vibration model with equal story height of 0.69m (a) Time history of rotation response (b) Single-sided magnitude spectrum (SSMS) of the rotation response.

#### 4.3.1.4. Coupled Vibration (Translation in the X-Direction and Torsion.)

The graphs below show SSMS and time history of rotation readings for the 0.5m, 0.6m and 0.69m equal story height models for coupled vibration (X-direction translation and torsion). In all cases, the mode with the PATCPMD, has a smaller peak SSMS reading. The SSMS peaks were reduced by 67.7%, 68.7% and 82.7% for 0.5m, 0.6m and 0.69m equal story heights respectively for torsion and by 52.6%, 75.2% and 82.5% for 0.5m, 0.6m and 0.69m equal story heights respectively for translation in the X direction by the addition of the PATCPMD. The positive damping effects of the PATCPMD are still significant. This demonstrates that the PATCPMD, without any tuning, can produce effective control on the Couple vibration even when the natural frequencies of the test structure are changed

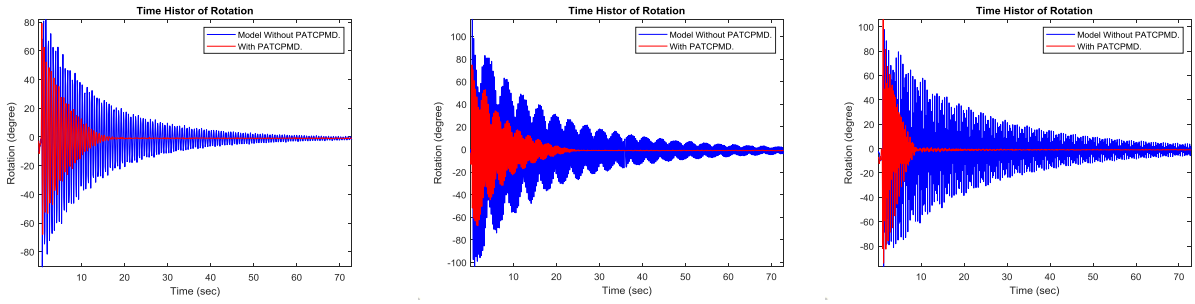


(a) (b) (c)

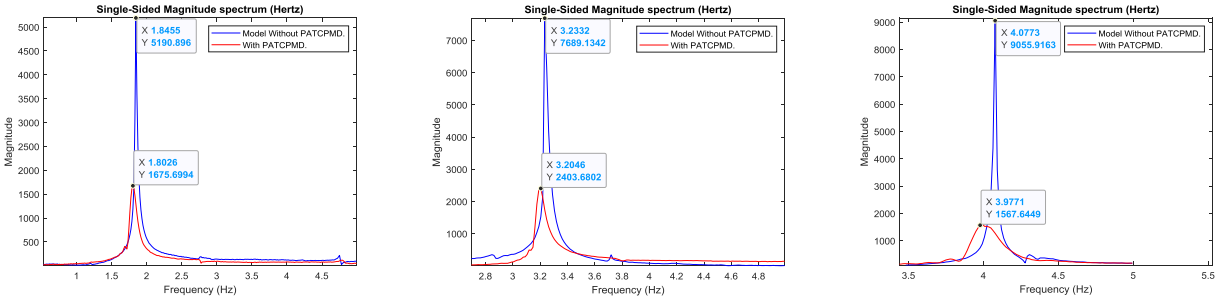


(d) (e) (f)

Figure 4.19. For free coupled(torsion and X axis) torsional vibration model with equal story height of 0.5m, 0.6m and 0.69m (a), (b) & (c) Time history of rotation response (d), (e) & (f) Single-sided magnitude spectrum (SSMS) of the rotation response respectively.

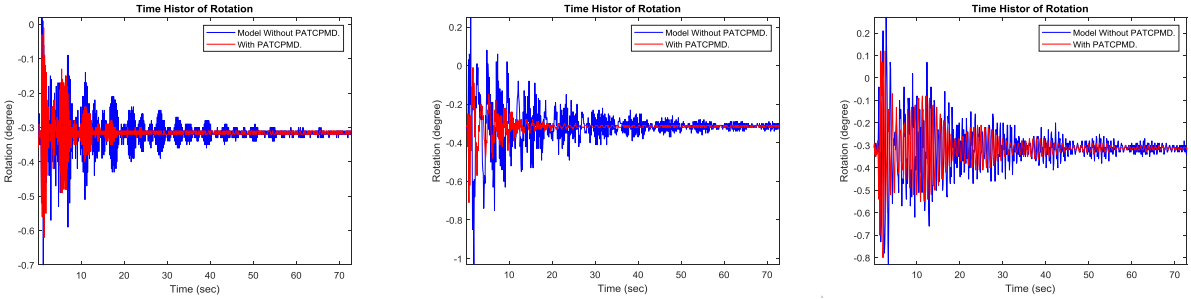


(a) (b) (c)

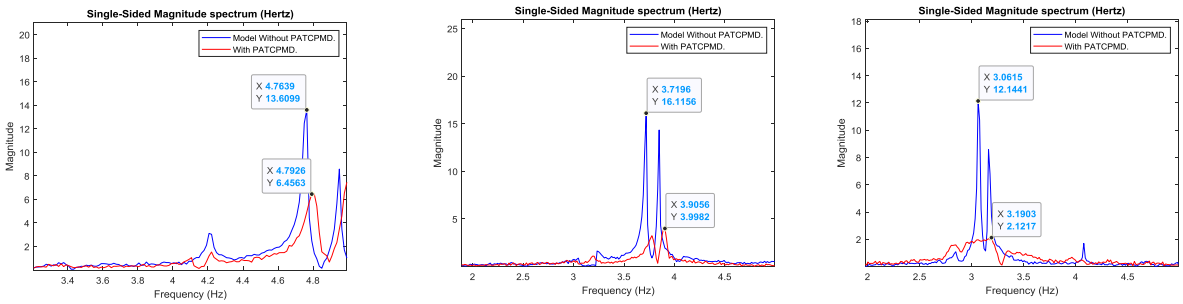


(d) (e) (f)

Figure 4.20. For free coupled(torsion and X axis) translational X axis vibration model with equal story height of 0.5m, 0.6m and 0.69m (a), (b) & (c) Time history of rotation response (d), (e) & (f) Single-sided magnitude spectrum (SSMS) of the rotation response respectively.

#### 4.3.1.5. **Coupled Vibration (Translational in the Y-Direction and Torsion.)**

The graphs below show SSMS and time history of rotation readings for the 0.5m, 0.6m and 0.69m equal story height models for coupled vibration (Y direction translation and tor-

sion). In all cases, the model with the PATCPMD, has a smaller peak SSMS reading. The SSMS peaks were reduced by 73.1%, 51.7% and 87.2% for 0.5m, 0.6m and 0.69m equal story heights respectively for torsion and by 62.3%, 72.4% and 87.6% for 0.5m, 0.6m and 0.69m equal story heights respectively for translation in the Y direction by the addition of the PATCPMD. The positive damping effects of the PATCPMD are still significant. This demonstrates that the PATCPMD, without any tuning or adjustment, can produce effective control on the Couple vibration (Translation in the Y-direction and Torsion) even when the natural frequencies of the test structure are changed.

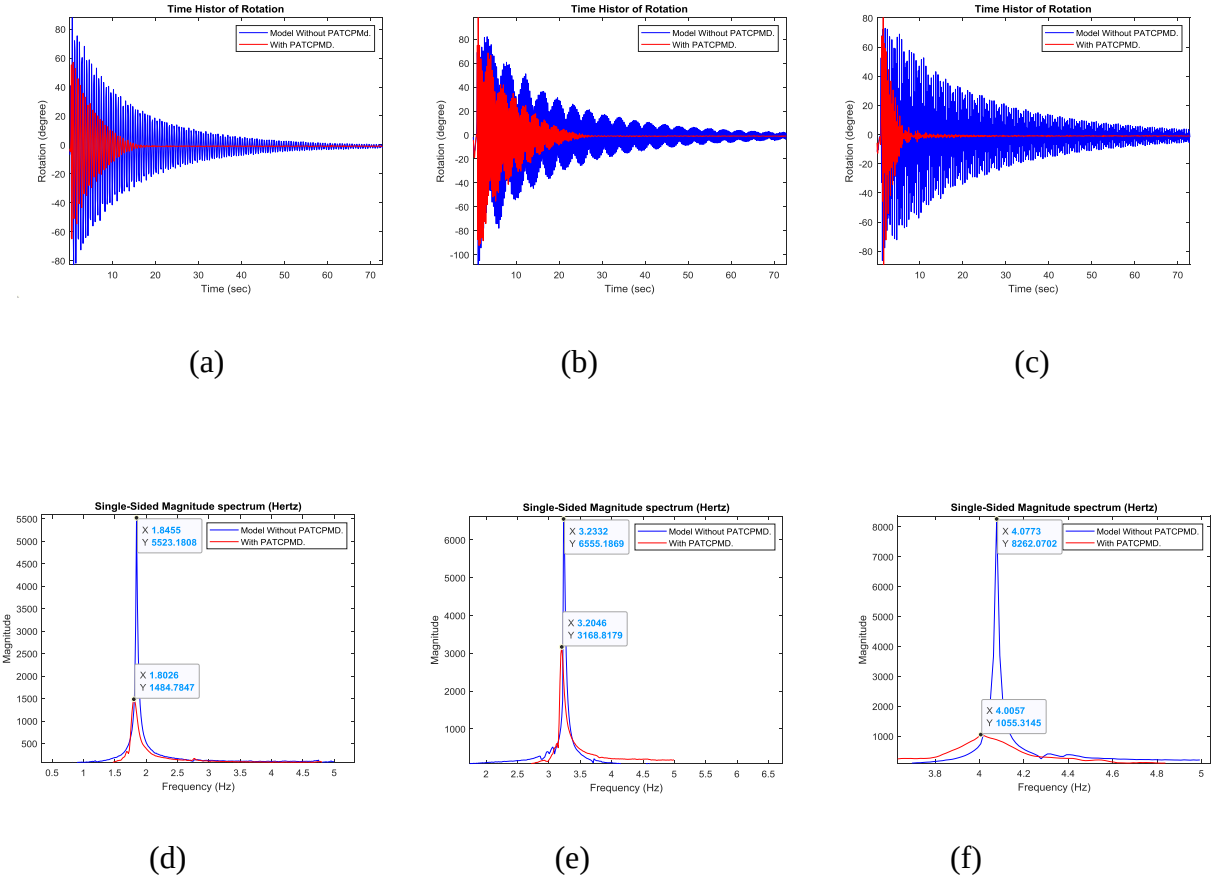


Figure 4.21. For free coupled(torsion and Y axis) torsional vibration model with equal story height of 0.5m, 0.6m and 0.69m (a), (b) & (c) Time history of rotation response (d), (e) & (f) Single-sided magnitude spectrum (SSMS) of the rotation response respectively.

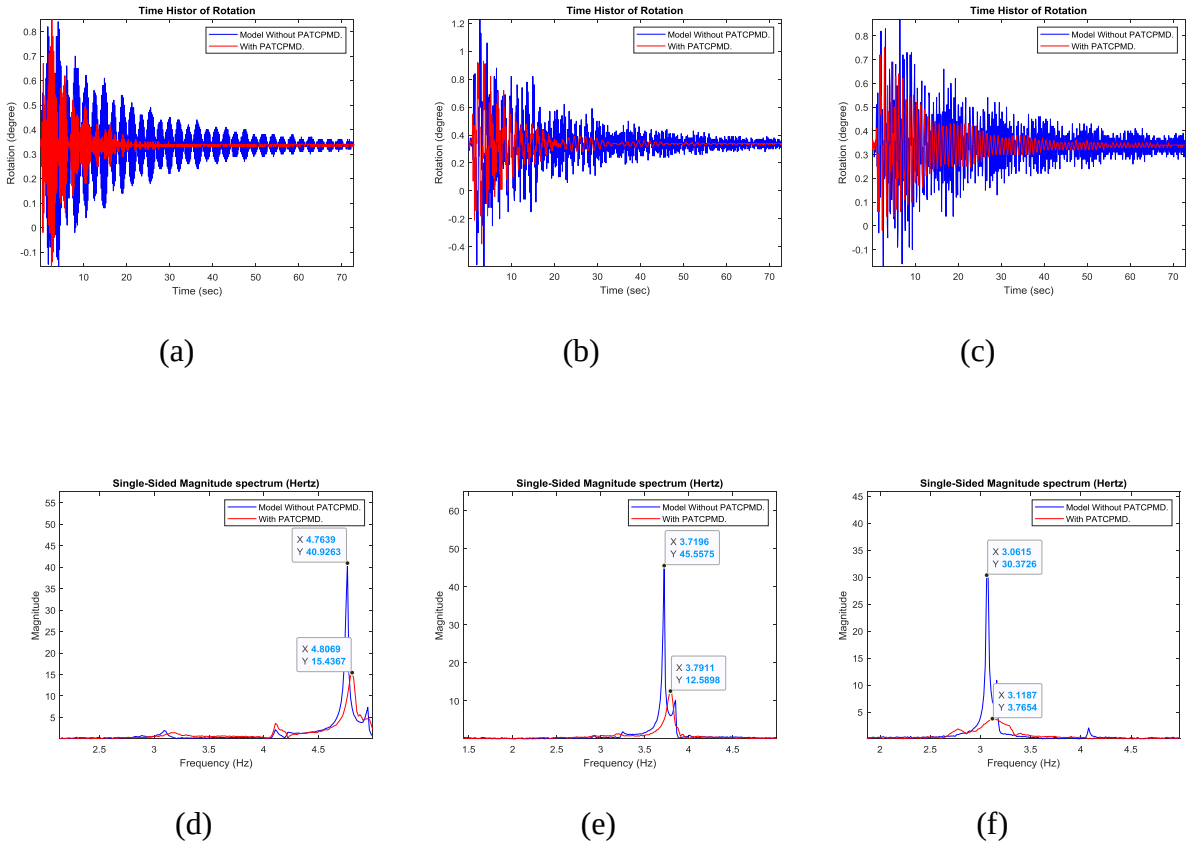


Figure 4.22. For free coupled(torsion and Y axis) translational Y axis vibration model with equal story height of 0.5m, 0.6m and 0.69m (a), (b) & (c) Time history of rotation response (d), (e) & (f) Single-sided magnitude spectrum (SSMS) of the rotation response respectively.

### 4.3.2. Forced Vibration.

#### 4.3.2.1. Translational Vibration in the X-Direction.

The same positive results that were observed in the free vibration tests were achieved in the forced vibration tests. As can be seen in Figure 33(a), (b) and (c) below, the SSMS peak is reduced by 50.0%, 51.1% and 88.5% for 50cm, 60cm and 69cm equal height respectively by the addition of the PATCPMD.

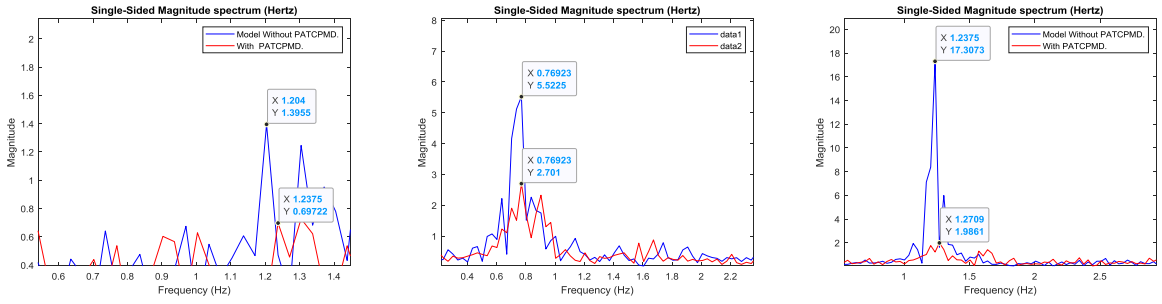

Figure 4.23. (a), (b) and (c) Single-sided magnitude spectrum (SSMS) of the acceleration response for forced translational vibration in the X direction for model with 0.5m, 0.6m and 0.69m equal height respectively.

#### 4.3.2.2. Translational Vibration in the Y-Direction.

Again, the positive results that were achieved in the free vibration tests were observed in the forced vibration tests for translational vibration in the Y-direction. The SSMS peak is reduced by 35.6%, 24.2% and 82.9% for 50cm, 60cm and 69cm equal height respectively by the addition of the PATCPMD.

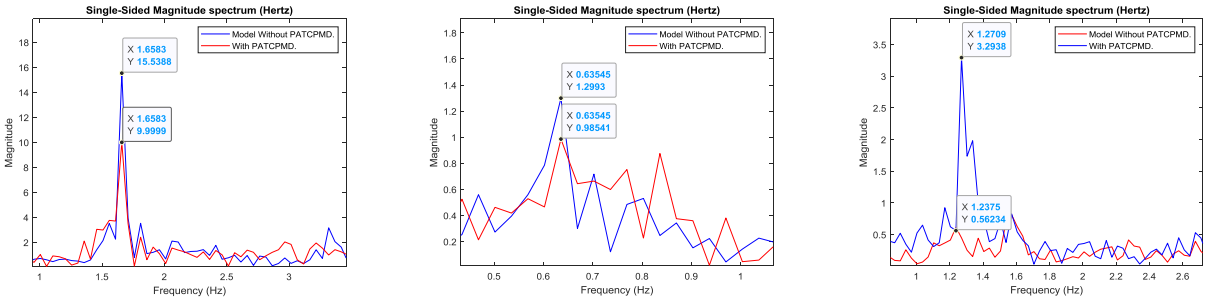


(a) (b) (c)

Figure 4.24. (a), (b) and (c) Single-sided magnitude spectrum (SSMS) of the acceleration response for forced translational vibration in the Y direction for model with 0.5m, 0.6m and 0.69m equal height respectively.

### 4.3.3. Summary and Conclusions.

By changing the height of the test model, its stiffness was altered and the natural frequencies were changed. The test results reveal that the PATCPMD reduced the model's vibration response considerably in every case, meaning that it worked effectively over a relatively wide frequency range without any tuning or specific adjustment. The SSMS peaks for translational vibration were reduced by between 49.4%-87.6% in every case, whilst the SSMS peaks for torsional vibration were reduced by between 51.3%-91.8% in every case for free vibration. Again the SSMS peaks for translational vibration were reduced by between 24.2%-88.5% in every case for forced vibration. In general, the test models subjected to free excitation attained higher levels of attenuation than those subjected to forced excita-

tion, as shown in the SSMS graphs above. This is due to the fact that during forced excitation fluctuation of frequency is observed as AC power supply is used.

## 4.4. Effects of Changing Model's Mass.

### 4.4.1. Free Vibration.

#### 4.4.1.1. Translational Vibration in the X-Direction.

The graphs below show the SSMS and time history of acceleration readings for the 14.104kg model and 14.7kg model respectively, for translational vibration in the X-direction. As can be seen, the natural frequency decreases with increasing model mass. The natural frequency for the 14.104kg model is 3.0151Hz and for the 14.7kg model is 2.9614Hz which is in agreement with the simulated results 3.359Hz and 3.346Hz respectively as shown earlier. In all cases, the model containing the PATCPMD, has a much smaller peak SSMS reading which again demonstrates the PATCPMD's effectiveness in controlling translational vibration over a relatively wide range of frequencies, without any tuning having taken place. The SSMS peak values were reduced by 79.8% and 88.5% by the addition of the PATCPMD for model mass 14.104kg and 14.7kg respectively. The time-history of acceleration graphs also demonstrate the PATCPMD's control effect.

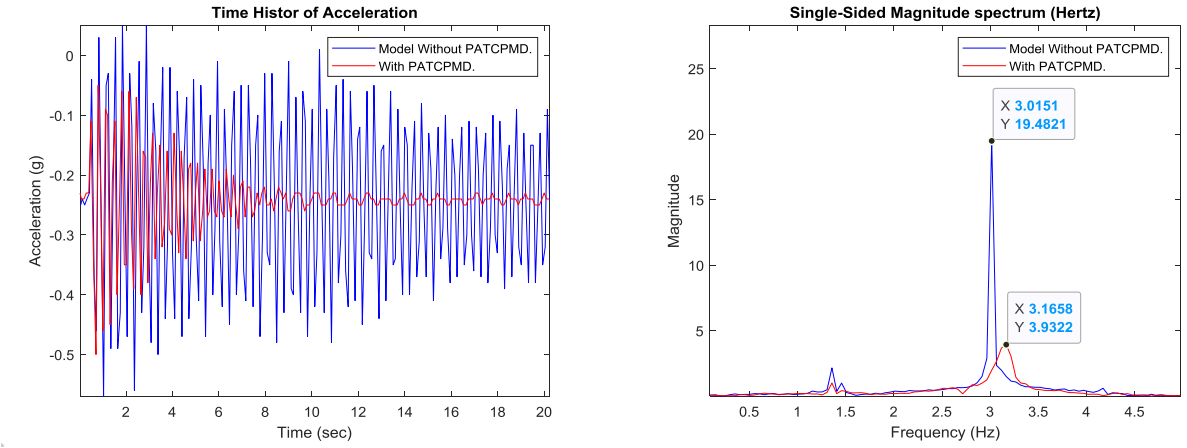


(a) (b)

Figure 4.25. For free translational vibration in X direction model with 14.104kg mass (a) Time history of acceleration response (b) Single-sided magnitude spectrum (SSMS) of the acceleration response.

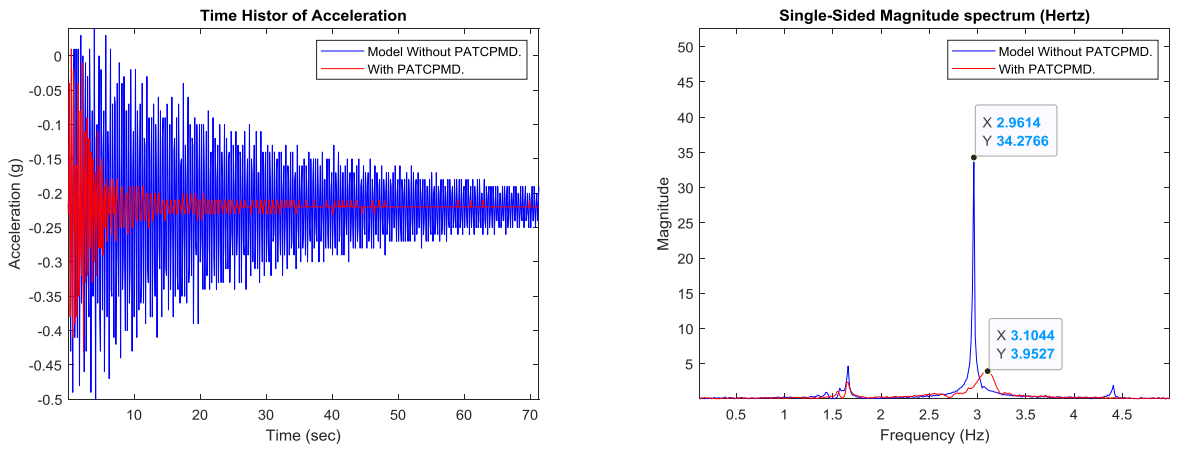


(a) (b)

Figure 4.26. For free translational vibration in X direction model with 14.7kg mass (a) Time history of acceleration response (b) Single-sided magnitude spectrum (SSMS) of the acceleration response.

#### 4.4.1.2. Translational Vibration in the Y-Direction.

The graphs below show the SSMS and time history of acceleration readings for translational vibration in the Y direction for each of the two model masses. The natural frequency for the 14.104kg model is 3.1156Hz and for the 14.7kg model is 3.0472Hz which is in agreement with the simulated results of 3.42Hz and 3.401Hz respectively as shown earlier. In all cases, the model containing the PATCPMD, has a much smaller peak SSMS reading which demonstrates the PATCPMD's effectiveness in controlling translational vibration over a relatively wide range of frequencies, without any tuning taken place. The SSMS peak values were reduced by 75.4% and 81.1% by the addition of the PATCPMD for model mass 14.104kg and 14.7kg respectively. The time history of acceleration graphs also demonstrate the PATCPMD's positive damping effects.

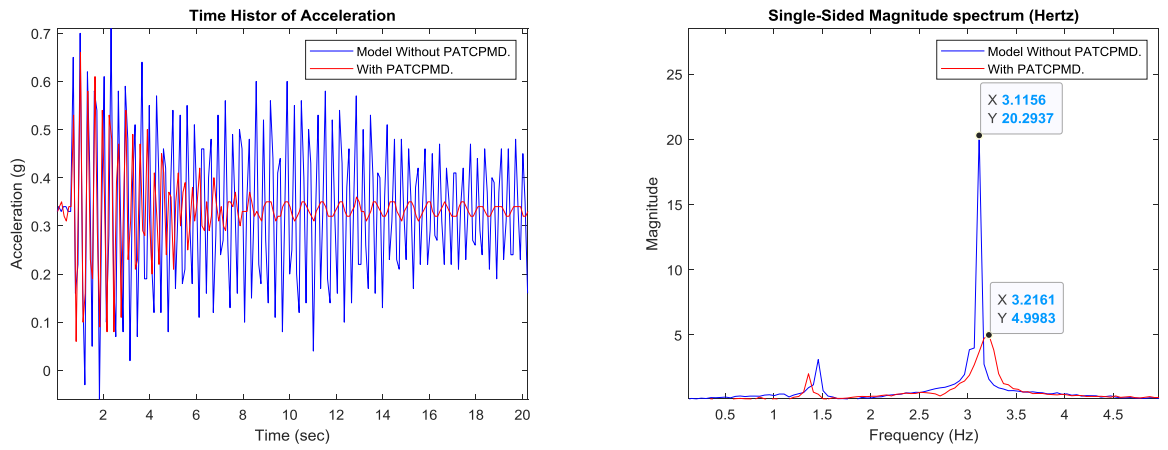


(a) (b)

Figure 4.27. For free translational vibration in Y direction model with 14.104kg mass (a) Time history of acceleration response (b) Single-sided magnitude spectrum (SSMS) of the acceleration response.

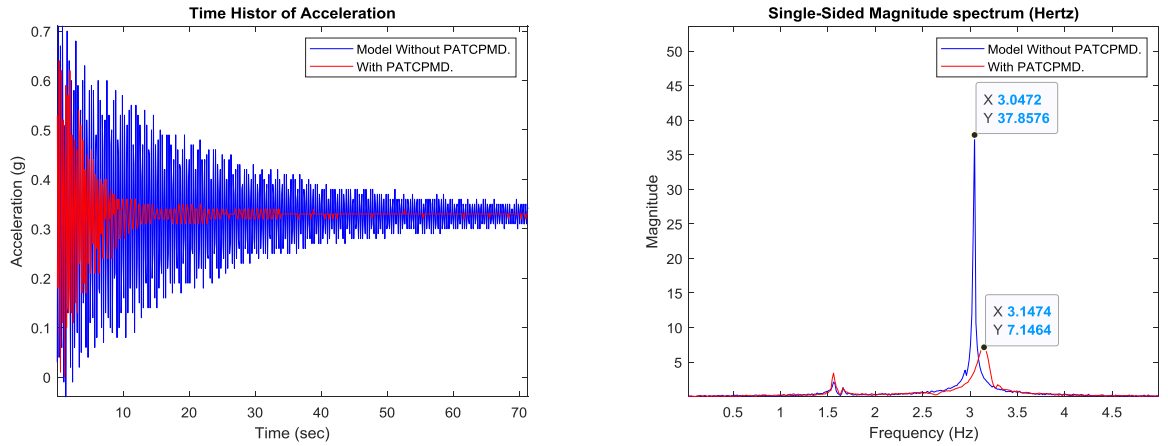


(a) (b)

Figure 4.28. For free translational vibration in Y direction model with 14.7kg mass (a) Time history of acceleration response (b) Single-sided magnitude spectrum (SSMS) of the acceleration response.

#### 4.4.1.3. **Torsional Vibration.**

The graphs below show the SSMS and time history of rotation readings for torsional vibration for each of the two model masses. As can be seen from the simulation results, the natural frequency for torsion decreases from 6.648Hz to 6.602Hz with increasing model mass. In all cases the addition of the PATCPMD reduced the SSMS reading by 91.9% and 67.7% for model mass 14.104kg and 14.7kg respectively, demonstrating the control effect of the PATCPMD on torsional vibration, without any tuning or adjustment.

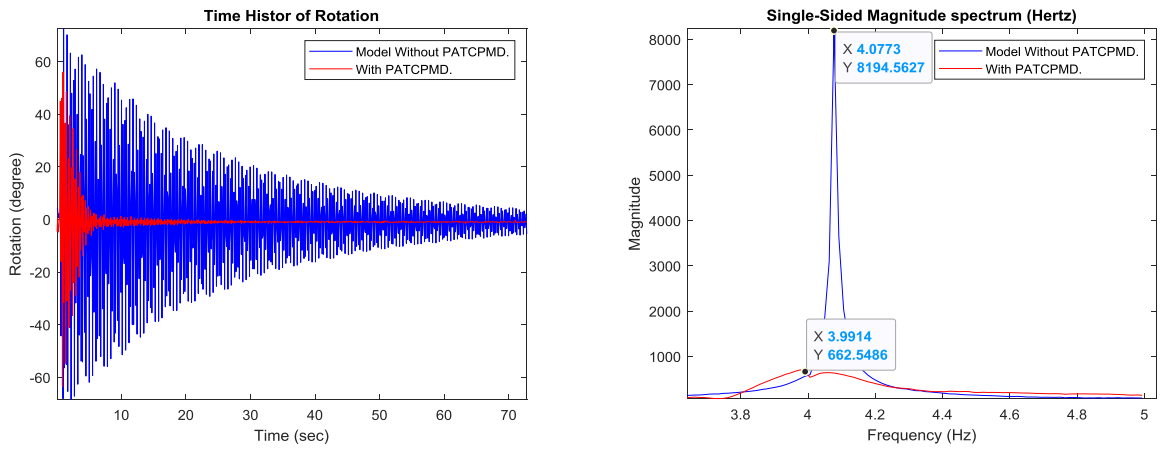


(a) (b)

Figure 4.29. For free torsional vibration model with 14.104kg mass (a) Time history of rotation response (b) Single-sided magnitude spectrum (SSMS) of the rotation response.

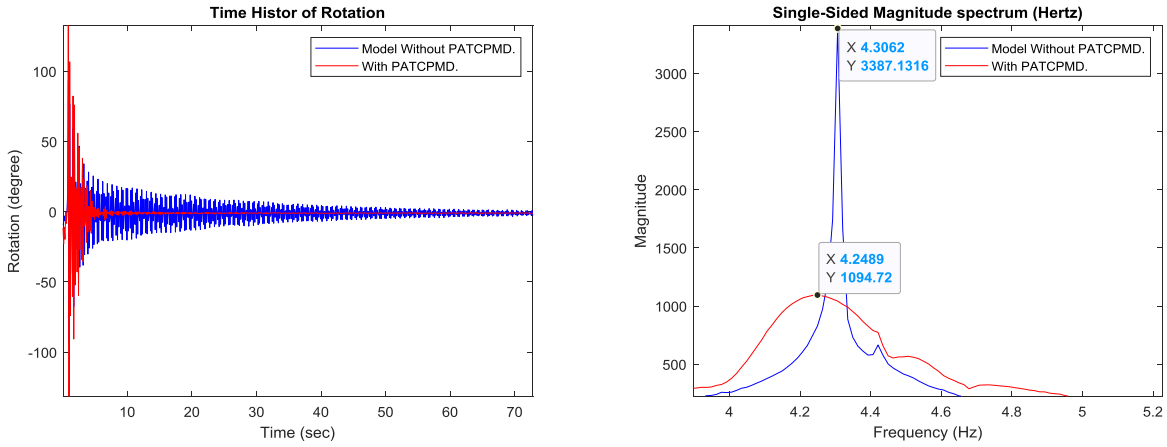


(c) (d)

Figure 4.30. For free torsional vibration model with 14.7kg mass (a) Time history of rotation response (b) Single-sided magnitude spectrum (SSMS) of the rotation response.

#### 4.4.1.4. Coupled Vibration (Translation in the X-Direction and Torsion.)

The graphs below show the SSMS and time history of rotation readings for the 14.104kg model and 14.7kg model respectively for coupled vibration (translation in the X-direction and torsion). In all cases, the model containing the PATCPMD reduced the SSMS reading by 82.7% and 62.5% for mass of 14.104kg and 14.7kg respectively for torsion and by 82.5% and 73.4% for mass of 14.104kg and 14.7kg respectively for translation in the X direction,

which demonstrates its effectiveness in controlling coupled vibration without having been tuned.

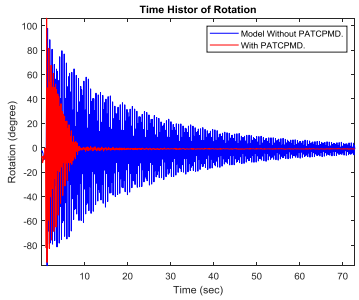


(a)

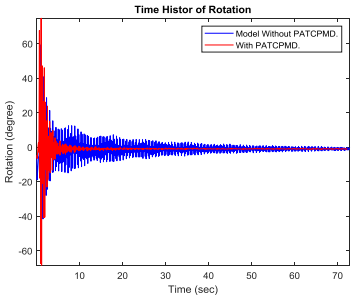


(b)

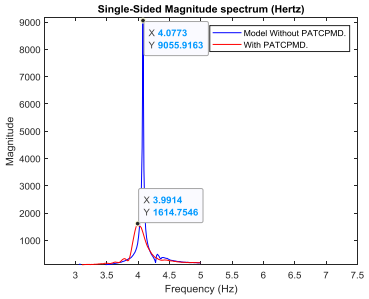


(c)

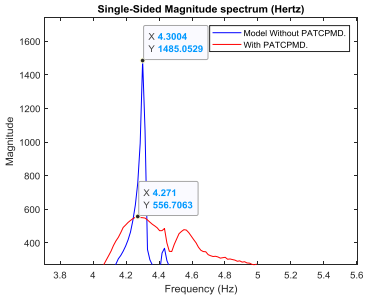


(d)

Figure 4.31. For free coupled(torsion and X axis) torsional vibration model with mass of 14.104kg and 14.7kg (a) & (b) Time history of rotation response (c) & (d) Single-sided magnitude spectrum (SSMS) of the rotation response.

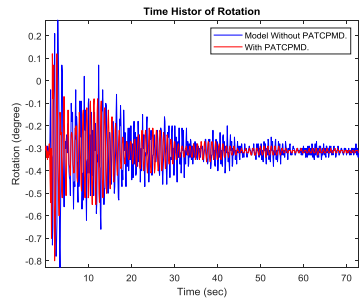


(a)

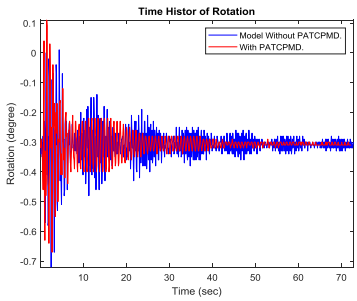


(b)

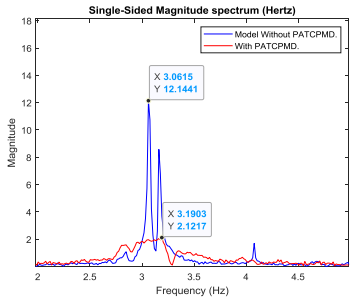


(c)

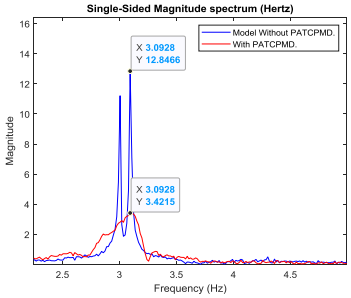


(d)

Figure 4.32. For free coupled (torsion and X axis) translational X axis vibration model with mass of 14.104kg and 14.7kg (a) & (b) Time history of rotation response (c) & (d) Single-sided magnitude spectrum (SSMS) of the rotation response.

#### 4.4.1.5. Coupled Vibration (Translational in the Y-Direction and Torsion.)

The graphs below show the SSMS and time-history of acceleration readings for the 14.104kg model and 14.7kg model respectively for coupled vibration (translation in the Y-direction and torsion). In all cases, the model containing the PATCPMD reduced the SSMS reading by 87.2% and 80.8% for mass of 14.104kg and 14.7kg respectively for torsion and by 87.6% and 88.6% for mass of 14.104kg and 14.7kg respectively for translation in the Y direction, which demonstrates its effectiveness in controlling coupled vibration.

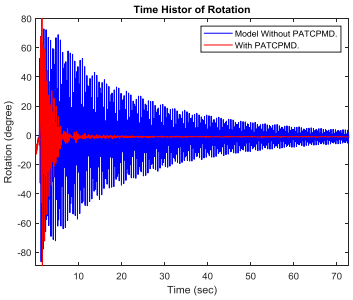


(a)

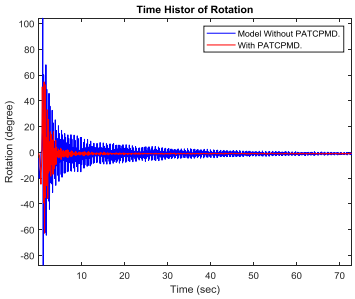


(b)

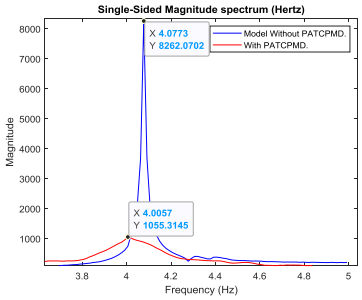


(c)

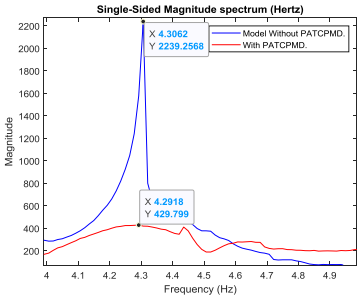


(d)

Figure 4.33. For free coupled(torsion and Y axis) torsional vibration model with mass of 14.104kg and 14.7kg (a) & (b) Time history of rotation response (c) & (d) Single-sided magnitude spectrum (SSMS) of the rotation response.

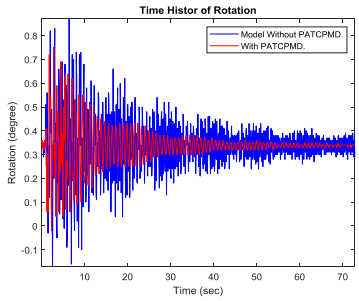


(a)

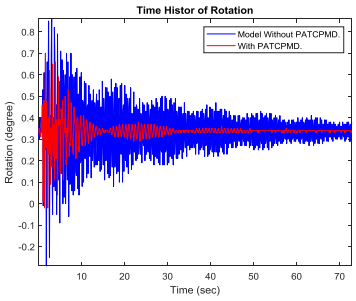


(b)

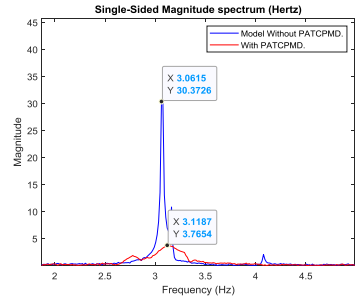


(c)

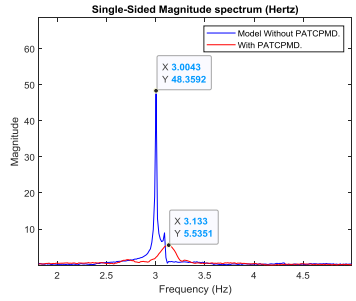


(d)

Figure 4.34. For free coupled (torsion and Y axis) translational in the Y axis vibration model with mass of 14.104kg and 14.7kg (a) & (b) Time history of rotation response (c) & (d) Single-sided magnitude spectrum (SSMS) of the rotation response.

### 4.4.2. Forced Vibration.

#### 4.4.2.1. Translational Vibration in the X-Direction.

The same positive results that were observed in the free vibration tests were achieved in the forced vibration tests. The SSMS peaks are reduced by 88.5% and 41.0% for model without and with mass respectively by the addition of PATCPMD.

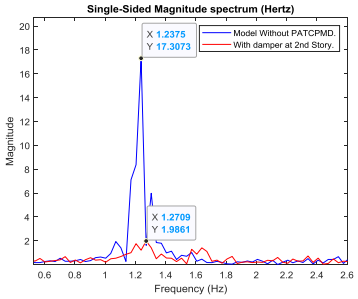


(a)

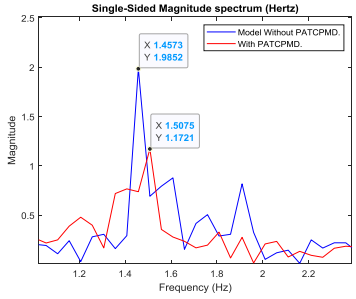


(b)

Figure 4.35. (a) and (b) Single-sided magnitude spectrum (SSMS) of the acceleration response for forced translational vibration in the X direction for model with mass 14.104kg and 14.7kg respectively.

#### 4.4.2.2. Translational Vibration in the Y-Direction.

As with the X-direction translational vibration, the tests for the Y-direction also produced the same positive results that were observed in the free vibration tests. The SSMS peaks are reduced by 82.9% and 56.6% without and with mass respectively by the addition of PATCPMD.


(a) (b)

Figure 4.36. (a) and (b) Single-sided magnitude spectrum (SSMS) of the acceleration response for forced translational vibration in the Y direction for model with mass 14.104kg and 14.7kg respectively.

### 4.4.3. Summary and Conclusions.

By changing the mass of the test model, the natural frequencies were altered. The test results reveal that the PATCPMD reduced the model's vibration response significantly in every case, meaning that it worked effectively over a relatively wide frequency range without any tuning or specific adjustment. The SSMS peak for translational vibration was reduced by at least 73.4% in every case, whilst the SSMS peak for torsional vibration was reduced by at least 62.5% in every case for free vibration test and the SSMS peak for translational vibration was reduced by greater than 41% in every case for forced vibration test. High accelerations and rotations were seen in the damped case soon after excitation in some instances; however these could be reduced immediately as time passes.

## 4.5. Effects of Changing PATCPMD Connection.

### 4.5.1. Free Vibration.

#### 4.5.1.1. Translational Vibration in the X-Direction.

In this first test, the model was given an initial 10mm displacement in the X-direction and released. The SSMS graph below demonstrates that the PATCPMD provides a postive damping effect for all the connection patterns considered. All of the connecting patterns of the PATCPMD provided high attenuation, reducing the SSMS peak values by 79.8%, 74.7% and 76.2% for pattern 1, pattern 2 and pattern 3 respectively. All of the cases again demonstrates the PATCPMD's capability of providing vibration control under very different conditions and without having been specifically tuned.

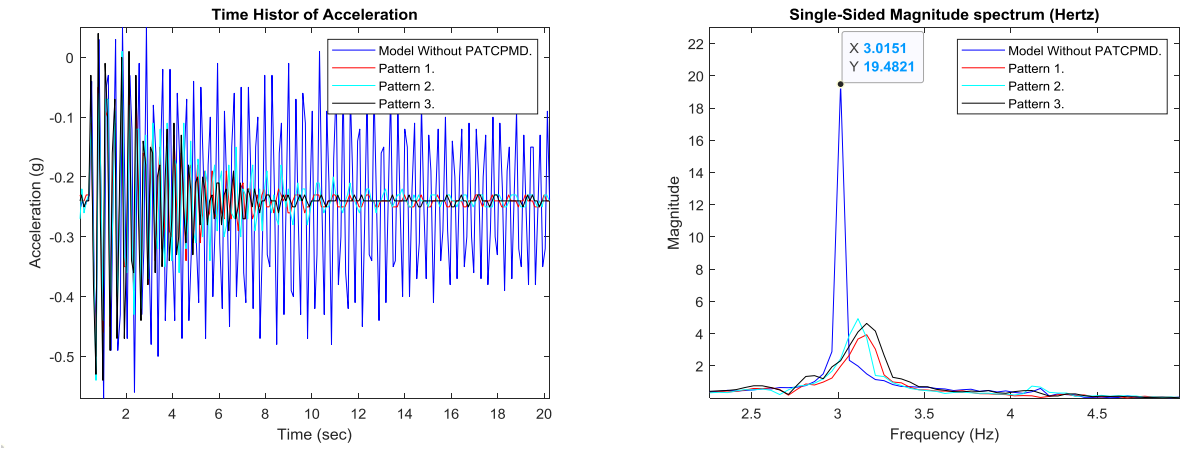


(a) (b)

Figure 4.37. For free translational vibration in X direction Model without PATCPMD and with Pattern 1, Pattern 2 and Pattern 3 (a) Time history of acceleration response (b) Single-sided magnitude spectrum (SSMS) of the acceleration response.

#### 4.5.1.2. Translational Vibration in the Y-Direction.

The model was then given an initial displacement of 10mm in the Y-direction and released. The SSMS graph below demonstrates that the PATCPMD provides a positive damping effect for all of the connection patterns considered, reducing the damped peak SSMS by 75.4%, 84.1% and 81.8% for pattern 1, pattern 2 and pattern 3 respectively, again demonstrating it's efficiency without having been tuned.

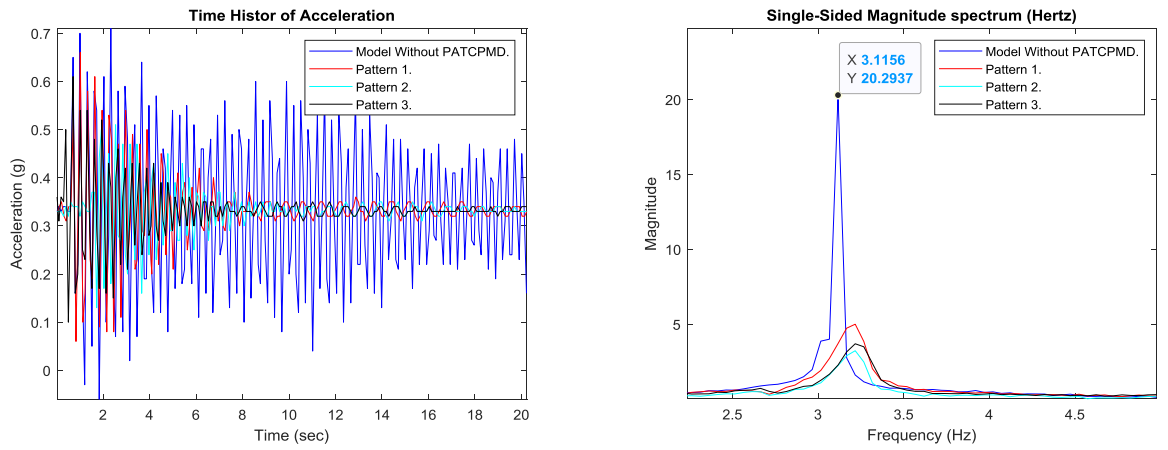


(a) (b)

Figure 4.38. For free translational vibration in Y direction Model without PATCPMD and with Pattern 1, Pattern 2 and Pattern 3 (a) Time history of acceleration response (b) Single-sided magnitude spectrum (SSMS) of the acceleration response.

#### 4.5.1.3. **Torsional Vibration.**

The model was then given an initial torsional displacement of 10mm.The SSMS graph below shows that the amount of attenuation provided by the PATCPMD for torsional vibration. The SSMS peaks were reduced by 91.4%, 18.0%, 70.9% by the addition of the PATCPMD for pattern 1, pattern 2 and pattern 3 respectively. This demonstrates that the connecting pattern can have a large impact on the level of attenuation achieved, however all of the configurations provided control, without any tuning of the PATCPMD.

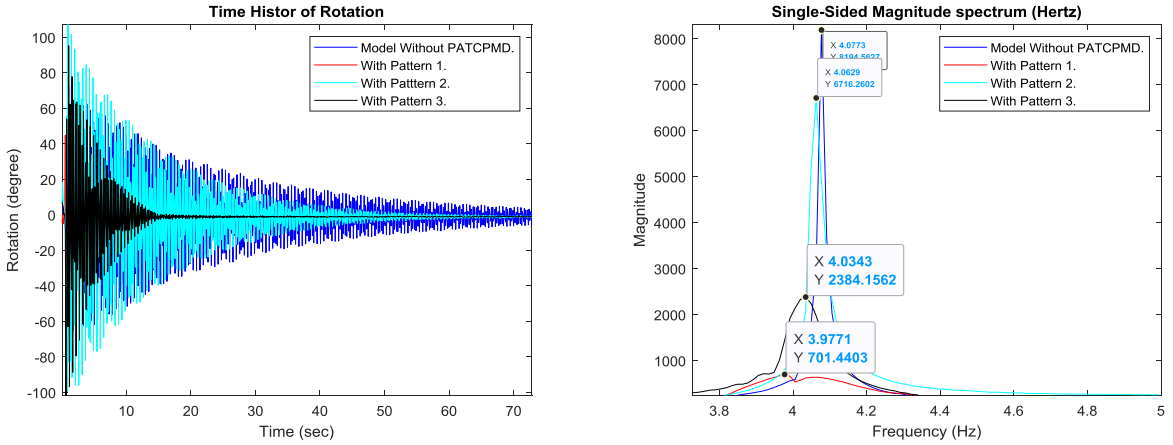


(a) (b)

Figure 4.39. For free torsional vibration model without PATCPMD and with Pattern 1, Pattern 2 and Pattern 3 (a) Time history of rotation response (b) Single-sided magnitude spectrum (SSMS) of the rotation response.

#### 4.5.1.4. Coupled Vibration (Translation in the X-Direction and Torsion.)

The model was then subjected to an initial coupled displacement (X-direction and torsion).The SSMS graph below shows that the amount of attenuation provided by the PATCPMD for coupled vibration. The SSMS peaks for the different patterns were reduced by 80.0%, 42.8%, 77.4% for torsion and by 82.5%, 64.2%, 71.6% for translation in the X direction by the addition of the PATCPMD for pattern 1, pattern 2 and pattern 3 respectively. This shows that the connecting pattern can have a large impact on the level of attenuation achieved, however all of the patterns provided control, without any tuning of the PATCPMD.

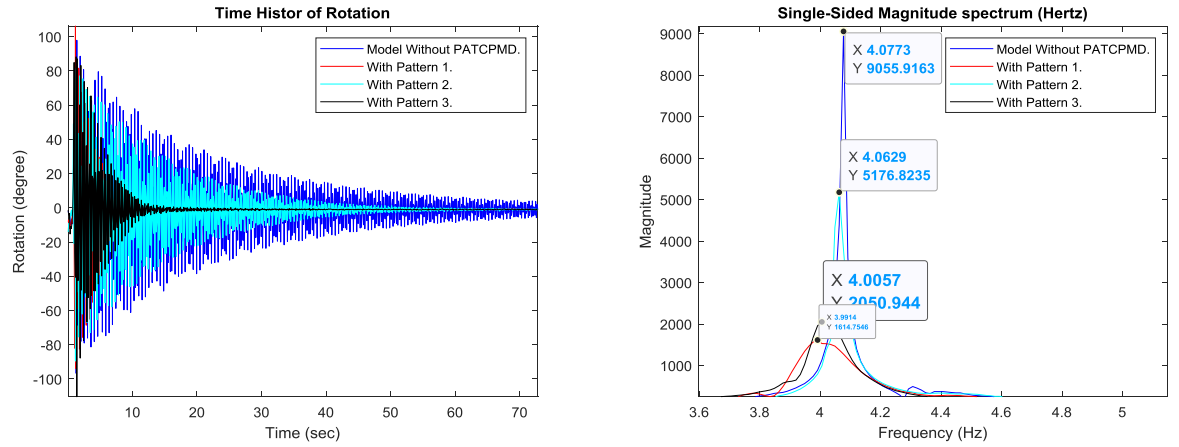


(a) (b)

Figure 4.40. For free coupled (torsion and X axis) torsional vibration model without PATCPMD and with Pattern 1, Pattern 2 and Pattern 3 (a) Time history of rotation response (b) Single-sided magnitude spectrum (SSMS) of the rotation response.

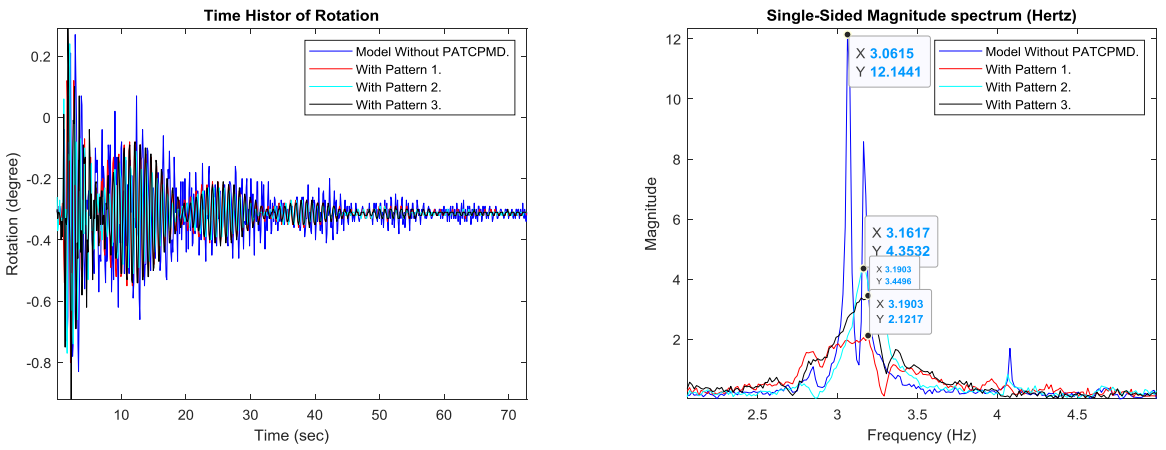


(a) (b)

Figure 4.41. For free coupled (torsion and X axis) translation in the X axis vibration model without PATCPMD and with Pattern 1, Pattern 2 and Pattern 3 (a) Time history of acceleration response (b) Single-sided magnitude spectrum (SSMS) of the acceleration response.

#### 4.5.1.5. Coupled Vibration (Translational in the Y-Direction and Torsion.)

The model was then subjected to an initial coupled displacement (Y-direction and torsion). The SSMS graph below shows that the amount of attenuation provided by the PATCPMD for coupled vibration. The SSMS peaks for the different patterns were reduced by 87.2%, 23.4%, 73.8% for torsion and by 87.5%, 66.8%, 85.6% for translation in the Y direction by the addition of the PATCPMD for pattern 1, pattern 2 and pattern 3 respectively. This demonstrates that the connecting pattern can have a large impact on the level of attenuation achieved, however all of the configurations provided control, without any tuning of the PATCPMD.

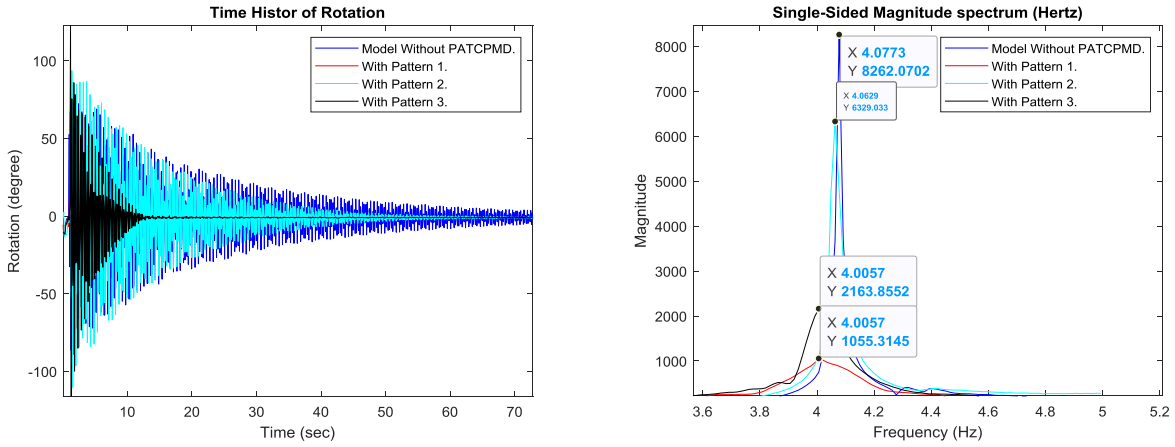


(a) (b)

Figure 4.42. For free coupled (torsion and Y axis) torsional vibration model without PATCPMD and with Pattern 1, Pattern 2 and Pattern 3 (a) Time history of rotation response (b) Single-sided magnitude spectrum (SSMS) of the rotation response.

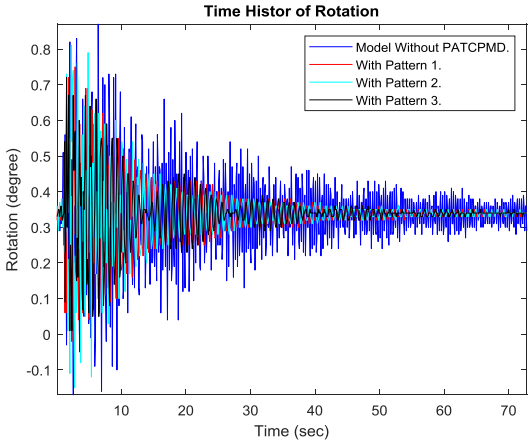


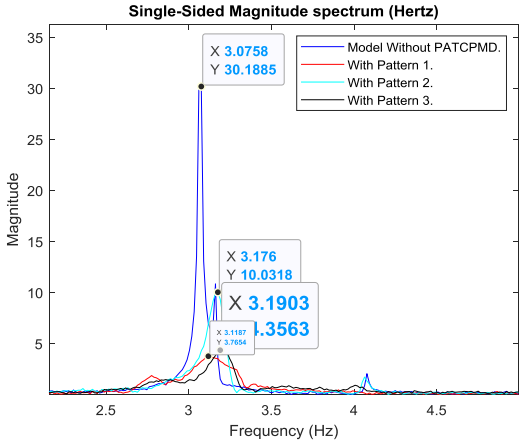


(a) (b)

Figure 4.43. For free coupled (torsion and Y axis) translation in the Y axis vibration model without PATCPMD and with Pattern 1, Pattern 2 and Pattern 3 (a) Time history of acceleration response (b) Single-sided magnitude spectrum (SSMS) of the acceleration response.

### 4.5.2. Forced Vibration.

#### 4.5.2.1. Translational Vibration in the X-Direction.

The model was placed on the shaking table for the forced vibration tests. As can be seen, the PATCPMD provided vibration attenuation for all of the pattern configurations considered. Once again, pattern 3 provided the least control, however the SSMS peak was still damped by 63.7% in this case.

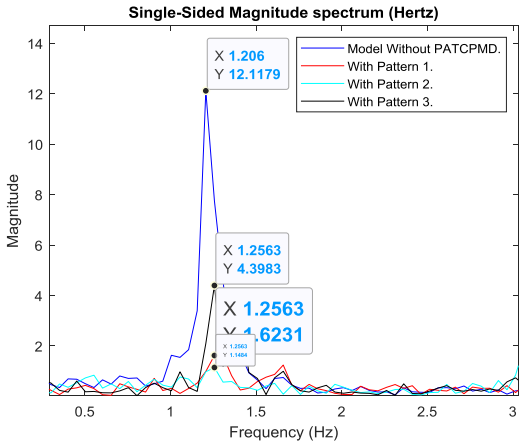

Figure 4.44. For force translation vibration in the X direction model without PATCPMD and with Pattern 1, Pattern 2 and Pattern 3 Single-sided magnitude spectrum (SSMS) of the acceleration response.

#### 4.5.2.2. Translational Vibration in the Y-Direction.

The model was placed on the shaking table in the Y-direction for these tests. As can be seen, the PATCPMD provided vibration attenuation for all of the connection patterns considered. Pattern 3 provided the least control with the SSMS peak being damped to by 23.5% in this case.

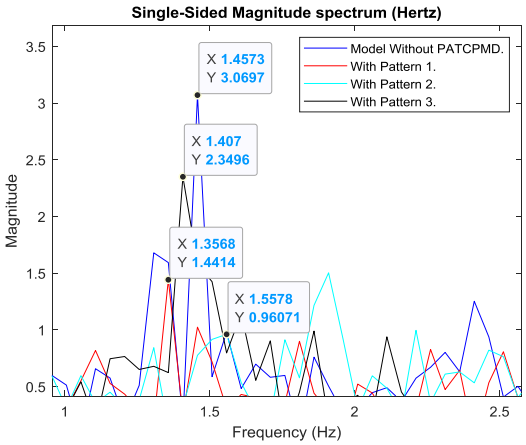


Figure 4.45. For force translation vibration in the Y direction model without PATCPMD and with Pattern 1, Pattern 2 and Pattern 3 Single-sided magnitude spectrum (SSMS) of the acceleration response.

### 4.5.3. Summary and Conclusions.

Most of the connection patterns provided significant attenuation to the translational, torsional and coupled vibrations of the test model. Two of the patterns, 2 and 3 provided less control than the pattern 1 in most of the tests. Pattern 3 represents the connection where all the eight ropes are suspended and stretched tightly. It is reasonable that this pattern did not provide high levels of attenuation as the PATCPMD was not free to move very much as it was suspended so tightly, and therefore it could not dissipate large amounts of energy. Pattern 2 represents the case where four middle centre of the ropes are suspended tightly. It is perhaps therefore understandable that the attenuation achieved is not very significant. Pattern 1 represents the connection where four corner ropes are suspended and four of them are moving back and forth. It is therefore might be the case where pattern 1 have achieved significant attenuation in most of the tests.

# Chapter 5.
# CONCLUSIONS AND RECOMMENDATIONS.

## 5.1. Conclusions.

The TMD is the most common control device found in the literature and has been the most widely implemented auxiliary device. It has however, a few drawbacks that have generated the need for research into improvements. The vibration attenuation device proposed herein, the PATCPMD, therefore tackles the issues of torsional and coupled vibration control and the detuning of the TMD. Based on the experimental study, the following conclusions can be drawn:

The experimental study results above show that the PATCPMD can successfully attenuate translational, torsional and coupled vibration when the PATCPMD is suspended both in the first and second story and subjected to free or forced excitations. The SSMS peak was reduced by between 48.0%-75.4% for translational as well as for torsional vibrations when the PATCPMD is suspended in the first story and by between 75.4%-90.0% for translational as well as for torsional vibrations when the PATCPMD is suspended in the second story which demonstrates its ability to effectively control all three types of excitation. However, as clearly observed from the result suspending the PATCPMD at the second story has a better effect than the first story.

The stiffness and mass of the test model were varied in the parameter tests, thereby altering the model's natural frequencies significantly. The SSMS peak for translational vibration was reduced by at least 49.4% in both cases, whilst the SSMS peak for torsional vibration was reduced by at least 51.3% in every case for free vibration test and the SSMS peak for translational vibration was reduced by greater than 24.2% in both cases for forced vibration test. This result shows that the PATCPMD continued to work effectively under the different conditions without being altered in any way; and it was therefore concluded that the PATCPMD is efficient under a relatively wide range of frequencies, without being tuned. This is a significant advantage over traditional TMDs which are often the subject of detuning due to changes in the structure's natural frequency, which can render the TMD ineffective.

The PATCPMD connection pattern to the test model were then altered, while keeping the model's other properties constant. Again, the PATCPMD provided significant attenua-

tion for most of the connecting patterns; however pattern 1 of the three patters provided more vibration control for most of the tests.

Generally, the preceding experimental results show that although the passive auto-tuning compound pendulum mass damper (PATCPMD) is a simple solution, it is robust, effective and versatile. It can effectively control translational, torsional and coupled vibration, without having been tuned, making it an alternative solution for many engineering applications.

Furthermore, torsional and coupled vibration have been more difficult to control in the past than translational vibration and often multiple dampers or active dampers are needed. The proposed PATCPMD, although a single passive auto-tuning damper, significantly reduced the torsional and coupled vibration of the test structure in the preceding tests.

### 5.2. Recommendations.

1) Although the attenuation provided by the PATCPMD in all cases reveals that specific tuning of the PATCPMD is not necessary, more research should be carried out to determine the PATCPMD more connection patterns and even the shapes which provide the optimum amount of vibration control.
2) The test model considered in the experimental study consisted of only a two storey steel frame model. The PATCPMD's effectiveness in a multiple storey structure should be investigated.
3) The research contained herein was based solely on experimentation of a test model. Further research needs to be carried out in order to develop practical design and optimisation guidelines in order for the PATCPMD to become a viable solution in real-life structures.
4) Although the test model was subjected to a single fluctuating frequency during the forced vibration tests, it was not subjected to a frequency sweep and an earthquake signal. Perhaps the PATCPMD's effectiveness under earthquake loading and frequency sweep should be subjects of further research.
5) Considering different parameters like different mass ratio, frequency ratio, damping ratio to obtain the optimum parameters should be a subject for further research, since in this thesis only single mass ratio, frequency ratio and damping ratio is considered.

## REFERENCES


1. Alexander Nicholas A, Schilder Frank(2009). "Exploring the Performance of non linear tuned mass damper" Journal of Sound and Vibration 319 pp 445–462
2. Chen, G., and Wu, J. (2003). "Experimental study on multiple tuned mass dampers to reduce seismic responses of a three- storey building structure." Earthquake Eng. Struct. Dyn. , Vol. 32, 793–810.
3. Chouw, Nawaw (2004) "Behaviour of soil-structure system with tuned mass damper during near-source earthquakes" 13th World Conference on Earthquake Engineering, Vancouver, B.C., Canada, August 1-6, 2004,Paper No. 1353.
4. Frahm, H.(1909).Device for Damping Vibrations of Bodies,U.S. Patent #989958.
5. Ghosha, A. and Basu, B. (2004) "Effect of soil interaction on the performance of tuned mass damper for seismic applications" Journal of Sound and Vibration 274 (2004) 1079–1090.
6. Islam, B. and Ahsan, R. (2012). "Optimization of Tuned Mass Damper Parameters Using Evolutionary Operation algorithm" 15 wcee, losboa 2012
7. Kwok, K. C. S., and Samali, B. (2006). "Performance of tuned mass dampers under wind loads". Engineering Structures , Vol. 17, No. 9, pp. 655~667, 1995.
8. Li, C. (2003). "Multiple active-passive tuned mass dampers for structures under the ground acceleration." Earthquake Eng. Struct. Dyn. ,32(6),949–964.
9. Li, Chunxiang and Liu, Yanxia (2002). "Active multiple tuned mass damper for structures under the ground acceleration " Earthquake engineering and structural dynamics earthquake engng struct. dyn. 2002; 31:1041–1052 (doi: 10.1002/eqe.136)
10. Lin, Chi-Chang, et al. "Vibration control of seismic structures using semi-active friction multiple tuned mass dampers." Engineering Structures 32.10 (2010): 3404-3417.
11. Lourenco,R. , Roffel, A. J. and Narasimhan, S. (2009) "Adaptive pendulum mass damper for the control of structural vibrations" Cansmart 2009 international workshop smart materials and structures 22 - 23 october 2009, montreal, quebec, Canada
12. Meaghan, C., (2013). "Experimental Investigations into a Passive Auto-Tuning Mass Damper." Faculty of Civil and Environmental Engineering, Johannesburg.
13. Nagashima Ichiro, Maseki Ryota, Asami Yutaka and Hirai Jun (2001) "Performance of hybrid mass damper system applied to a 36-storey high-rise building" Earthquake engineering and structural dynamics earthquake engng struct. dyn. 2001; 30:1615–1637 (doi: 10.1002/eqe.84)

14. Padmabati, S., (2015). "Experimental and numerical study on tuned mass damper in controlling vibration of frame structures." Department of Civil Engineering, NIT Rourkela.
15. Sadek, Fahim et al(1997). "A method of estimating the parameters of tuned mass dampers for seismic applications". Earthquake engineering and structural dynamics, vol. 26, 617-635
16. Saidi, I . ,Mohammed, A. D. and Gad, E. F., (2007). "Optimum Design for Passive Tuned Mass Dampers Using Viscoelastic Materials" Australian Earthquake Engineering Society Conference
17. Samali, Bijan and Al-Dawod, Mohammed (2003). "Performance of a five-storey benchmark model using an active tuned mass damper and a fuzzy controller" Engineering Structures 25 (2003) 1597–1610.
18. Setareh Mehdi(2001). "Application of semi-active tuned mass dampers to base-excited systems" Earthquake engineering and structural dynamics earthquake engng struct. dyn. 30:449-462.
19. Wong K.K.F(2008) "Seismic Energy Dissipation of Inelastic Structures with Tuned Mass Dampers" Journal of Engineering Mechanics, Vol. 134, No. 2 77)
20. Wu J., Chen G. and Lou M., "Seismic Effectiveness of Tuned Mass Dampers Considering Soil-Structure Interaction", Earthquake Engineering and Structural Dynamics, Vol. 28, No. 11, pp. 1219-1233, 1999.

**APPENDIX A:** ETABS 2016 SIMULATIONS.

**Changing the Model's Stiffness:**

***Model with 0.6m equal story height.***

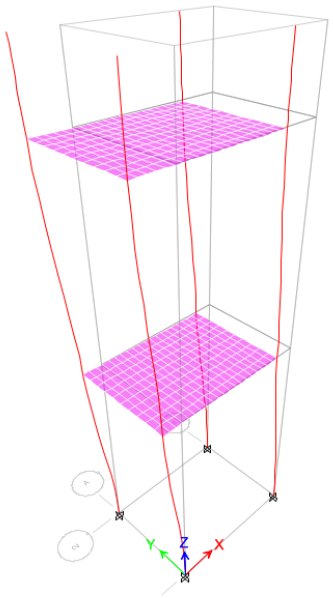


fx=4.011Hz.

Figure A-1: Translational vibration in the X direction.

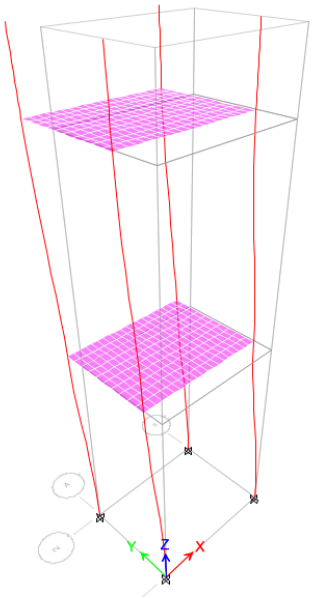


fy=4.091Hz.

Figure A-2: Translation vibration in the Y direction.

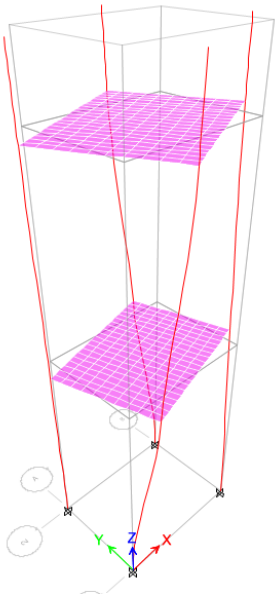


fz=7.47Hz.

Figure A-3: Torsional vibration.

***Model with 0.5m equal story height.***

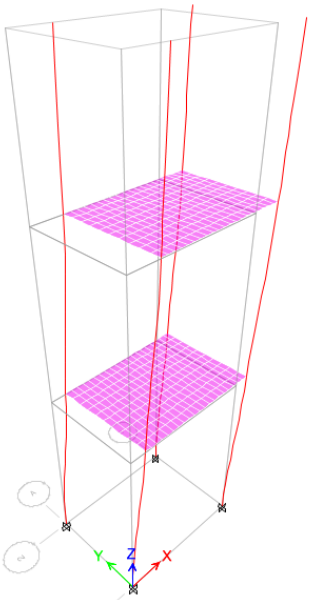


fx=5.035Hz.

Figure A-4: Translational vibration in the X direction.

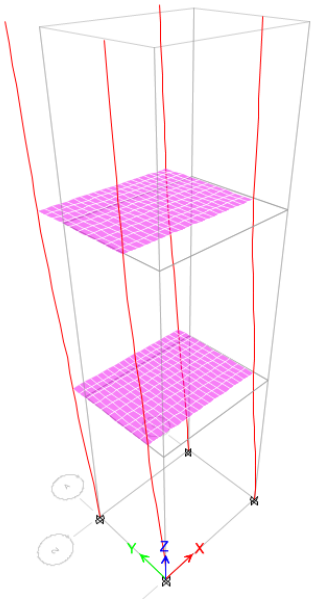


fy=5.15Hz.

Figure A-5: Translation in the Y direction.

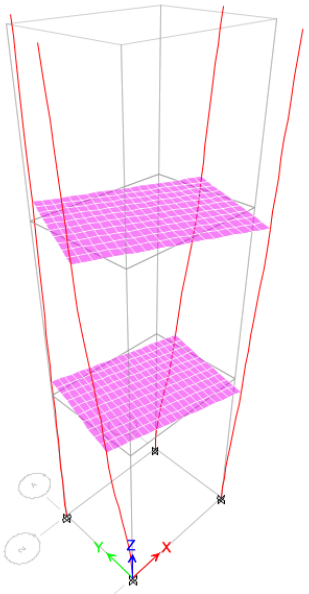


fz=8.701Hz.

Figure A-6: Torsional vibration.

**Changing the Model's Mass:**

***Model with 4.104kg mass.***

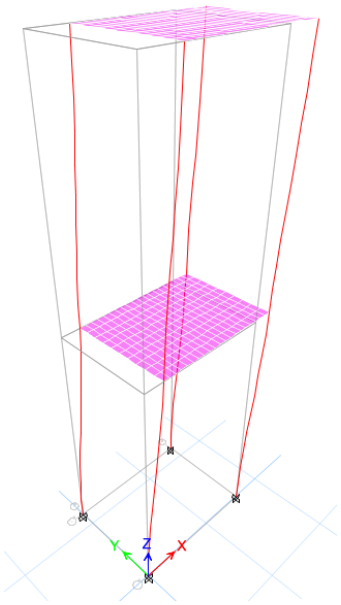


fx=3.359Hz.

Figure A-7: Translation in the X direction.

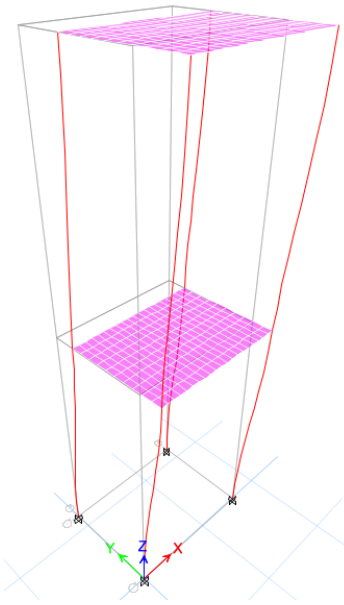


fy=3.42Hz.

Figure A-8: Translation in the Y direction.

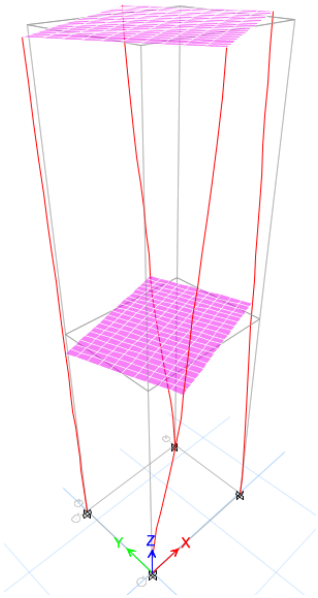


fz=6.648Hz.

Figure A-9: Torsional vibration.

***Model with 4.7kg mass.***

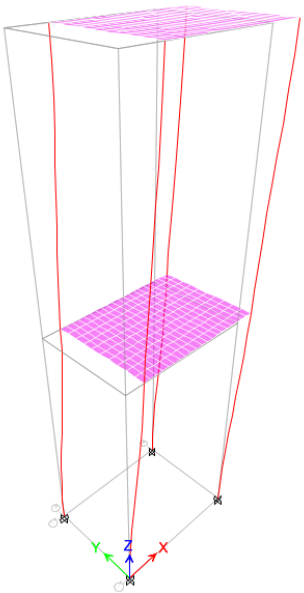


fx=3.346Hz.

Figure A-10: Translation in the X direction.

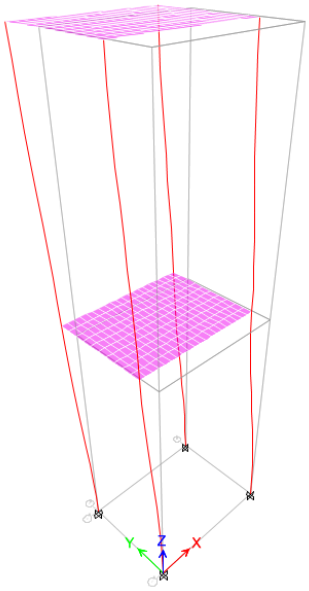


fy=3.401Hz.

Figure A-11: Translation in the Y direction.

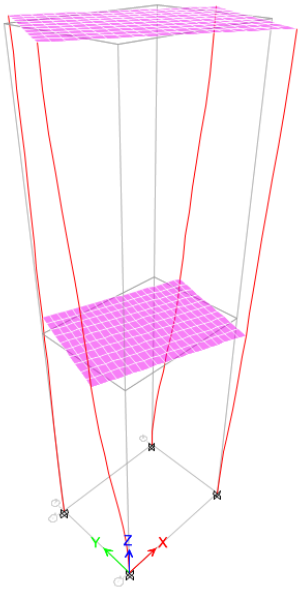


fz=6.602Hz.

Figure A-12: Torsional vibration.

## **APPENDIX B:** PHOTOGRAPHS


Figure B-1: Model with PATCPMD is suspended at the second story.


Figure B-2: Model with PATCPMD is suspended at the first story.

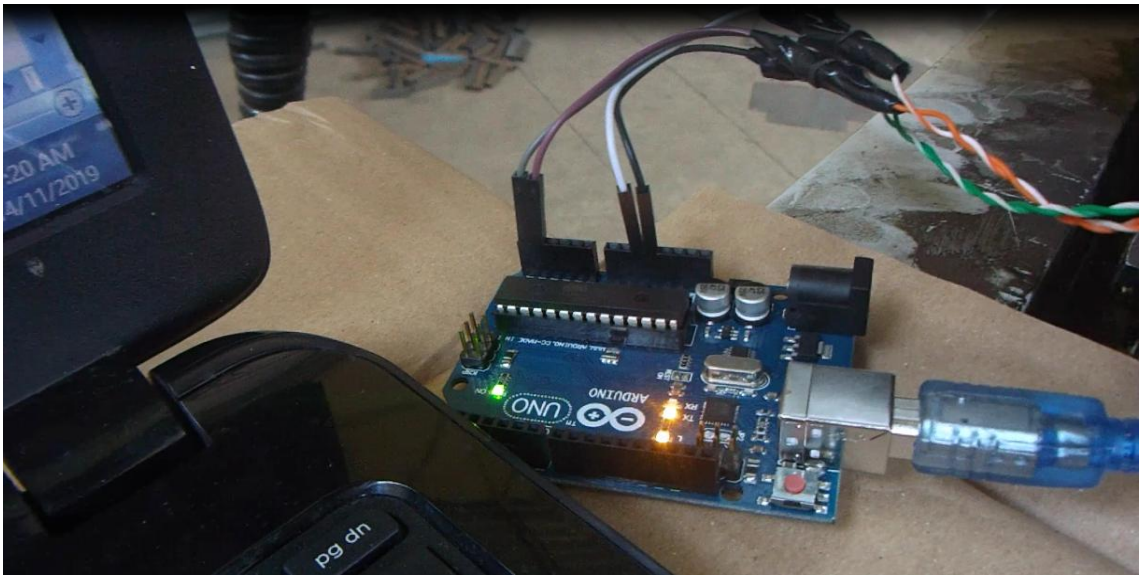


Figure B-3: Arduino Uno Board while taking data.


Figure B-4: Gyro accelerometer attached to the top story for taking the data**.**

Figure B-5: Tachometer while reading the Rpm.


Figure B-6: Dimmer Switch for controlling the speed of the Hammer Drill.


Figure B-7: Dial gauge for measuring initial displacement for free vibration.


Figure B-8: A close up photo of PATCPMD.